American Mineralogist, Volume 109, pages 2037–2051, 2024

Evaluation of the Rietveld method for determining content and chemical composition of inorganic X-ray amorphous materials in soils

Sileola Joseph Akinbodunse[1], Kristian Ufer[2], Reiner Dohrmann[2,3], and Christian Mikutta[1,*,†]

[1]Soil Mineralogy, Institute of Mineralogy, Gottfried Wilhelm Leibniz University Hannover, Callinstr. 3, D-30167 Hannover, Germany
[2]Federal Institute for Geosciences and Natural Resources (BGR), Stilleweg 2, D-30655 Hannover, Germany
[3]State Authority of Mining, Energy and Geology (LBEG), Stilleweg 2, D-30655 Hannover, Germany

Abstract

Inorganic X-ray amorphous materials (iXAMs) such as vitreous phases, minerals having an insufficient number of repeating structural units to diffract X-rays, and inorganic solids with exclusively structural short-range order are ubiquitous in soils and are relevant for numerous environmental processes but are notoriously difficult to identify and quantify. To test for the quantification and chemical composition of iXAMs in soil, we prepared four mineral mixtures containing quartz, calcite, feldspars, and clay minerals in different proportions typical of soils and amended them with 10–70 wt% iXAMs in the form of a 1:1 weight mixture of ferrihydrite and opal-A. We quantified these iXAMs in mineral mixtures by analyzing powder X-ray diffraction (PXRD) data using the Rietveld method and compared the results for different sample preparation techniques (conventional and spray drying) based on the internal standard method in Rietveld analysis. The mineral mixtures were also analyzed for their chemical composition by X-ray fluorescence (XRF) spectrometry, and mass-balance calculations combining Rietveld and XRF data were carried out to estimate the chemical composition of iXAMs in mineral mixtures. Both sample preparation methods showed no significant difference in determined iXAM contents and yielded accurate results for iXAM contents within ±3 wt% at the 95% confidence level (2σ). The relative accuracy deteriorated with decreasing iXAM content but remained below 10% for iXAM contents >10 wt% (mean = 3%). The precision of iXAM content quantification in mineral mixtures prepared by spray drying was slightly better, though statistically equivalent to the conventionally prepared mixtures (2σ = 1.49 and 1.61 wt%). The average precision of both sample preparation methods was ±2 wt% at the 95% confidence level. Levels of detection and quantification of iXAMs in spray-dried mineral mixtures containing 1–10 wt% iXAMs were estimated at 0.8 and 4.0 wt%, respectively. The chemical composition of iXAMs in terms of major oxides was accurately assessed by mass-balance calculations with average relative errors for nominal SiO_2 and Fe_2O_3 contents of 9.4 and 4.3%, respectively (range = 0.02–54.7%). Even though adsorbed H_2O and structural H_2O/OH^- as quantified by the loss on ignition comprised an important portion of the iXAMs (15.3 wt%), their LOI in mineral mixtures as derived from mass-balance calculations could only be quantified with an average relative error of 67.2% (range = 1.30–371%). We conclude that iXAMs in soil and related geomaterials present at levels >4 wt% can be quantified by Rietveld analysis of PXRD data with an accuracy of ±3 wt% at best. Combined results of Rietveld and XRF analyses can yield accurate results for the chemical composition of iXAMs within a relative error of 10% for major oxides, provided iXAM contents exceed 10 wt%, and the content and chemical composition of all crystalline mineral phases are accurately assessed. The results presented in this study lay the foundation to explore iXAM contents and chemical compositions in soils and to examine their impact on soil physicochemical properties and biogeochemical element cycles.

Keywords: Amorphous inorganic materials, soil, XRD, Rietveld analysis, mineralogical budgeting, quantification, chemical composition

Introduction

In condensed matter physics, materials science, and chemistry, the term "amorphous" (from the Greek *a*, without, *morphé*, shape, form) refers to the absence of structural long-range order, that is, periodicity, in a substance. In contrast, the term "X-ray amorphous" defines solids that do not exhibit sharp Bragg peaks in their X-ray diffraction (XRD) patterns but are only detectable by broad diffuse X-ray scattering peaks. X-ray amorphous materials (XAMs) in soils are present as organic and inorganic compounds. The former materials, consisting of particulate and mineral-associated organic matter, are usually removed prior to XRD analysis using oxidants such as H_2O_2, NaOCl, and $Na_2S_2O_8$ (Jones et al. 2000; Mikutta et al. 2005a; Manaka 2006; Zabala et al. 2007). Therefore, XAMs recognizable in XRD patterns of soil samples by elevated background levels are predominantly inorganic in nature. Inorganic X-ray amorphous materials (iXAMs) in soil encompass a great variety of materials, such as vitreous

* Corresponding author E-mail: c.mikutta@mineralogie.uni-hannover.de
† Open access: Article available to all readers online.

0003-004X/24/0012–2037$05.00/DOI: https://doi.org/10.2138/am-2023-9240

phases, minerals having an insufficient number of repeating structural units to diffract X-rays, so-called "short-range order," "non-crystalline," or "poorly crystalline" minerals, and inorganic solids with variable elemental composition and exclusively structural short-range order, often termed "mineraloids." Paracrystalline minerals like allophane, imogolite, ferrihydrite, and vernadite as well as amorphous silica, are typical examples (Higashi and Ikeda 1974; Taylor and Schwertmann 1974; Walker 1983; Parfitt and Childs 1988; Wada 1989; Kaufhold et al. 2010; Lessovaia et al. 2014, 2016; Casetou-Gustafson et al. 2018; Zahoransky et al. 2022). The quantities of iXAMs in soils vary a lot. They can range from 1 to 15 wt% in fine earth fractions (<1 or <2 mm) (Zabala et al. 2007; Tamppari et al. 2012; Lessovaia et al. 2014; Casetou-Gustafson et al. 2018), and generally increase with decreasing particle size (Manaka 2006). The highest iXAM contents of up to 47–77 wt% have been reported for clay fractions (<2 μm) (Jones et al. 2000; Manaka 2006; Lessovaia et al. 2016).

Inorganic XAMs in soils play a crucial role in biogeochemical processes such as mineral weathering, carbon sequestration, and sorption reactions of nutrients and pollutants (Hellmann et al. 1990; Filgueiras et al. 2002; Abollino et al. 2011; Ruiz-Agudo et al. 2012, 2016; Basile-Doelsch et al. 2015; Bazilevskaya et al. 2018). They also exert great influence on soil physical properties such as aggregate stability, permeability, cementation, friability, porosity, surface area, bulk density, clay dispersion, and hydraulic conductivity (Goldberg 1989; Jones et al. 2000; Sanborn et al. 2011; Rawlins et al. 2013; Lehtinen et al. 2014; Totsche et al. 2018). Therefore, accurate and fast methods for quantitative analysis of iXAMs in soils and their parent materials are of great importance. Wet-chemical extractions have become the standard in soil science for selective removal of iXAMs from soils. The most commonly employed extractants are acid ammonium oxalate, ascorbic acid, disodium 4,5-dihydroxy-1,3-benzenedisulfonate (Tiron), ethylenediaminetetraacetic acid (EDTA), and hydroxylamine (NH_2OH) (Rennert 2019; Rennert et al. 2021). The main drawback of wet-chemical extractions to quantify the total iXAMs content in soil is their element selectivity and ability to even dissolve crystalline materials (Schwertmann and Taylor 1972; Higashi and Ikeda 1974; Taylor and Schwertmann 1974; Walker 1983; Parfitt and Childs 1988; Wada 1989; Dohrmann et al. 2002; Kaufhold et al. 2010). In contrast, powder X-ray diffraction (PXRD) in combination with extraction methods offers much greater potential for iXAMs quantification in soils than chemical extractions alone. In fact, PXRD has long been used to study amorphous solids in soils (Brydon and Shimoda 1972; Ross 1980; Schwertmann et al. 1982; Blank and Fosberg 1991). In its simplest application, PXRD is used to identify XAMs by the appearance of "amorphous humps" in X-ray diffractograms (DeMumbrum 1960; Blank and Fosberg 1991). In more sophisticated applications, PXRD patterns are recorded before and after treatment of soil solids with selective extractants used to dissolve specific amorphous components (Schwertmann et al. 1982; Kodama and Wang 1989). Far fewer studies utilized quantitative phase analysis (QPA) of PXRD data, which relies on the fact that the abundance of a crystalline phase relates to the intensity of its X-ray diffraction peaks. Among QPA methods, the Reference Intensity Ratio (RIR) method, also known as the matrix flushing method after Chung (1974), has been most popular in past decades. The method involves comparing the intensity of one or more peaks of a phase with the intensity of a peak of an internal standard (usually the 113 reflections of corundum) in a 50:50 wt% mixture. Once the RIR values for all crystalline phases in a sample are known, the weight abundance can be determined for every crystalline phase in the sample. The content of XAMs can then be calculated by a difference to 100 wt%. The RIR method may suffer from the effects of variable chemistry and preferred crystal orientation since only one or a series of reflections are used.

A second method for QPA of PXRD data involves fitting of XRD standard patterns to an entire sample pattern to obtain quantitative abundances of both crystalline and X-ray amorphous components ("full profile fitting method," FULLPAT) (Chipera and Bish 2002, 2013). This method is similar to the RIR method, but utilizes the entire diffraction pattern rather than single reflections, including the background signal that contains information of sample composition and matrix effects. Here, amorphous or disordered materials are accounted for by their individual XRD patterns (standard patterns). Full profile fitting thus allows the direct quantification of XAMs without the addition of an internal standard and has proven successful in QPA of unknown samples (Omotoso et al. 2006; Casetou-Gustafson et al. 2018). Similar to the RIR method, this type of QPA requires that phases used as standards do not significantly differ from the respective phases in the sample in terms of chemical composition and structure and that standards and samples are measured with the same instrument settings.

The third popular method of QPA of PXRD data are the Rietveld method, which involves constructing a model consisting of crystal structures of all component phases (Rietveld 1969; Bish and Post 1993). In Rietveld analyses, differences between observed and simulated diffraction patterns are minimized by varying model parameters, including scale factors related to phase abundances, unit-cell parameters, and crystallite size and strain-broadening parameters for each phase. Atomic positions and site occupancies can be varied as well (Rietveld 1969). The method provides information on all phases with long-range order (crystalline phases), while XAMs are quantified as one entity. Usually, the Rietveld method normalizes the summed mass fractions of crystalline components to unity. Determining the amorphous fraction in a sample involves blending the sample with a known amount of an internal standard (e.g., corundum). If amorphous material is present, the Rietveld-determined mass fraction of this standard is higher than the amount mixed with the sample. The mass fraction of XAMs is then calculated as:

$$\text{XAMs} = (S_R - S)/[S_R\,(1 - S)] \quad (1)$$

where S is the mass fraction of the standard and S_R is the Rietveld-determined standard mass fraction. Once the mass fraction of XAMs is determined, the final mass fraction of a crystalline component X_i is calculated from a Rietveld refinement of the non-spiked sample according to:

$$X_i = (1 - \text{XAMs}) \times X_{iR} \quad (2)$$

with X_{iR} being the Rietveld-determined mass fraction of phase X_i (Jones et al. 2000).

Although the Rietveld method has some advantages over the conventional quantitative XRD approach (RIR method) in terms

of accuracy and detection limits (Rietveld 1969; Bish and Post 1993; Gualtieri 2000; Chipera and Bish 2002), it also suffers from limitations such as missing or inappropriate structure models and inadequate sample preparation. The first point is of particular importance because clay minerals in soils are often disordered. Over the past 15 years, Ufer and coworkers developed disorder models for full-pattern Rietveld refinement of PXRD data of expandable clay minerals of the smectite group (Ufer et al. 2004; Szczerba and Ufer 2018; Wang et al. 2018) and later of interstratified expandable clay minerals such as illite-smectite (Ufer et al. 2012a). Recently, first models were developed for hydroxy-interlayered minerals (HIMs) present in acidic soils (Dietel et al. 2019a, 2019b). Provided appropriate structure models are available, sub-optimal sample preparation for PXRD analysis can also spoil the outcome of Rietveld refinements. Conventional sample preparation often leads to preferred orientation, which occurs when the crystallites in a powder are not randomly oriented, that is, when there is a greater probability for the crystallites to be oriented in one particular direction than in the others. The effect of preferred orientation, which is most pronounced for phyllosilicate minerals, can be corrected to some extent in Rietveld refinements by mathematical functions such as the March function or spherical harmonics (Dollase 1986; Ahtee et al. 1989; Järvinen 1993; Gualtieri 2000). However, the best way to counteract preferred orientation is to avoid it. For this, spray drying of powdered samples has been proven to be very effective for QPA (Smith et al. 1978; Hillier 1999a).

Despite advanced knowledge on the application of quantitative PXRD to geomaterials, information on Rietveld-determined quantities of iXAMs in soils is limited (Weidler et al. 1998; Jones et al. 2000; Manaka 2006; Zabala et al. 2007; Tamppari et al. 2012; Lessovaia et al. 2014, 2016; Casetou-Gustafson et al. 2018). Perhaps the most obvious reason for this is the complex sample matrix, which can contain highly disordered clay minerals, solid solutions, and structurally well-defined minerals with distinct crystal defects. These factors may limit the success of Rietveld analysis for iXAM quantification in soils. Poor accuracy and/or reproducibility of iXAM contents determined by Rietveld analysis inevitably leads to high uncertainty in the chemical composition of iXAMs. The chemical composition of iXAMs can be estimated from mass-balance calculations using the Rietveld-based iXAM content and information on chemical sample composition as obtained by, for example, X-ray fluorescence (XRF) spectrometry ("balance sheet method" or "mineral budgeting approach") (Jones et al. 2000; Andrist-Rangel et al. 2006). To this end, XRF-based oxide contents and loss on ignition (LOI) are first assigned to each crystalline phase, usually by assuming ideal stoichiometry, and the non-explained oxide fractions and LOI are then assigned to XAMs (Jones et al. 2000; Cesarano et al. 2018).

To date, we are lacking information on the basic performance of the Rietveld method for iXAM quantification in soils. Data on analytical method characteristics such as accuracy, precision, and limits of detection and quantification are not currently available. Because of this lack of knowledge, it is currently impossible to reliably assess the abundance and chemical composition of iXAMs in soils, establish quantitative relationships with physicochemical soil properties, and evaluate iXAM fractions dissolved by routinely applied wet-chemical soil extractions. Thus, our main objectives were: (1) to evaluate the accuracy and precision of iXAM quantification using Rietveld analysis of PXRD data; (2) to determine Rietveld-based detection and quantification limits for iXAMs in soils or related geomaterials; (3) to test for the optimal way of PXRD sample preparation for iXAM quantification; and (4) to examine the accuracy of chemical iXAM analysis by mass-balance calculations using Rietveld and XRF data ("balance sheet method"). To achieve these goals, we prepared mineral mixtures of increasing complexity, consisting of quartz, feldspars, carbonate, and clay minerals, averaging the mineralogical composition of several European soils. We amended these mixtures with known amounts of synthetic iXAMs and analyzed their content and chemical composition by Rietveld refinements of PXRD data and XRF spectrometry. For PXRD measurements, the mixtures were either spray-dried or directly loaded into XRD sample holders ("conventional sample preparation"). The obtained information serves as a framework for future Rietveld-based PXRD studies on iXAMs in soils or related geomaterials that address their ecological relevance.

Materials and methods

Samples and sample preparation

Minerals of this study were obtained from the mineral collection of the Federal Institute for Geosciences and Natural Resources (BGR), Hannover, Germany. Table 1 summarizes information on their origin, nominal formulas, and purity. Five to seven minerals were mixed in different mass ratios (Table 2) to approximate the average mineral composition of European Luvisols developed on loess (without

Table 1. Description of minerals used in this study

Mineral	Source	Nominal formula	Purity (%)[a]
Albite (Ab)	Tørdal, Norway	$NaAlSi_3O_8$	94.3
Calcite (Cal)	Hunan, China	$CaCO_3$	100
Chlorite (Chl)	Korshunovskaia mine, Russia	$(Mg,Fe^{2+})_5Al(Si_3Al)O_{10}(OH)_8$	100
Corundum Baikalox CR1 (Crn)	Baikowski (synthetic)	Al_2O_3	100
Ferrihydrite (Fhy)	Own lab (synthetic)	$Fe_2O_3{\cdot}9H_2O$	100
Illite-smectite, disordered (Ilt-Sme)[b]	Korom Hill, Hungary	$(Ca,K)(Al,Mg,Fe)_2(Si,Al)_4O_{10}(OH)_2$	96.9
Kaolinite, disordered (Kln)	Mauretania	$Al_2Si_2O_5(OH)_4$	97.0
Labradorite (Lb)	Bekily, Madagascar	$(Ca,Na)(Si,Al)_4O_8$	100
Opal-A (Opl)	China (synthetic)	$SiO_2{\cdot}11H_2O$	100
Orthoclase (Or)[c]	Stavern, Norway	$(K,Na)(Al,Si)_4O_8$	100
Quartz (Qz)	Unknown	SiO_2	100
Smectite, disordered (Sme)[d]	Milos, Greece	$(Al,Fe,Mg)_2(Si,Al)_4O_{10}(OH)_2$	93.2

[a] Without intrinsic or induced amorphicity during sample preparation. Minor phases: Ab, 5.7% quartz; Ilt-Sme, 3.1% quartz; Sme, 3.5% orthoclase and 3.3% albite; Kln, 2% anatase, <1% quartz, <1% rutile, and <1% svanbergite.
[b] Illite-smectite mixed-layer mineral with R3 ordering with traces of quartz similar to the illite-smectite F4 sample in Ufer et al. (2012b).
[c] Mixture of K and Na feldspars (microcline and plagioclase 16an).
[d] Smectite-dominated (93.2%) bentonite with traces of feldspars (Ufer et al. 2008).

TABLE 2. Mineral mixtures and their respective compositions (wt%)

Mixture[a]	Qz	Feldspars			Cal	Chl	Ilt-Sme	Kln	Sme
		Ab	Lb	Or					
A	60	10	–	10	–	5	10	5	–
B	50	10	–	10	10	–	15	5	–
C	40	–	–	15	20	5	20	–	–
D	20	–	10	20	–	5	20	15	10

[a] A: loess composition without calcite, B: loess composition with calcite, C: composition of a marly glacial till, D: granite composition. Ab = albite; Cal = calcite; Chl = chlorite; Ilt-Sme = illite-smectite; Kln = kaolinite; Lb = labradorite; Or = orthoclase; Qz = quartz; Sme = smectite.

carbonate) (Tarrah et al. 2000; Pospíšilová et al. 2021), Cambisols or Podzols developed on granite (Gudmundsson and Stahr 1981; Žigová et al. 2013), and a marly glacial till (Scheffer and Schachtschabel 2010). Before blending minerals together, each mineral was ground to a particle size <5 µm (~4 mL mineral plus 10 mL ultrapure water; resistivity: ≥18.2 MΩ cm) for 5–10 min with a McCrone micronizing mill using cylindrical ZrO_2 grinding elements. The minerals were then oven-dried at 60 °C. One part of the mineral mixtures was spiked with an internal standard (30 wt% corundum) to determine their inherent amorphicity and the amorphicity induced by grinding and mixing. The other part was blended with different proportions of synthetic iXAMs (10–70 wt%) consisting of ferrihydrite and opal-A in a 1:1 mixture by weight and then spiked with an internal standard before proceeding with PXRD analysis. Ferrihydrite and opal-A were used because they are important soil iXAMs, which can constitute >10 wt% of soil clay fractions (Mikutta et al. 2005b; Lessovaia et al. 2016). As an internal standard, we used corundum Baikalox CR1, a high-grade, crystalline reference material with a particle size of <2 µm. The low amorphicity potentially associated with the corundum was insignificant when compared to the amount of amorphous material in the mineral mixtures.

Appropriate amounts of internal standard blended with samples are crucial for Rietveld-based quantification of XAMs, since the amorphous fraction is calculated from the Rietveld-determined mass fraction of the standard. Various spike levels have been used in the past. Hillier (2000) used 10 wt% for an artificial sandstone mixture containing 19.8 wt% glass, while Ufer et al. (2008) utilized a spike of either 10 or 20 wt% for smectite-rich bentonites. According to Jones et al. (2000), a smaller spike (10 wt%) is a good choice for samples with high amorphous content and a higher spike level (50 wt%) is better suited for samples with low amorphous contents, while a spike level of 30 wt% was considered a good compromise for soils with amorphous content of 28–77%. This is due to the need to find a compromise between the best possible sensitivity and over-dilution of the sample by the standard (Jones et al. 2000; Westphal et al. 2009). Therefore, we also used a spike level of 30 wt% to obtain an adequate signal from the standard for the different iXAM concentrations in the mineral mixtures.

For conventional PXRD sample preparation, minerals were mixed in an agate mortar with ethanol as a grinding aid. Another portion of mineral mixtures was spray-dried following Hillier (1999a) to minimize the effect of preferred orientation on QPA results. For this, we employed the rocket-shaped spray dryer manufactured by the James Hutton Institute (Aberdeen, Scotland, U.K.). Before spray drying, mineral powders were mixed with ultrapure water containing 0.5 wt% polyvinyl alcohol ($[-CH_2CH(OH)-]_n$, molecular weight: ~22 kDa, VWR) and 0.1 wt% of 1-octanol [$CH_3(CH_2)_7OH$, Thermo Fisher Scientific]. The solid-to-liquid ratio (w/v) ranged from 1:3 to 1:5. Polyvinyl alcohol helped to bind the dried product, while 1-octanol prevented foaming during solution dispersion and the formation of air bubbles in the dried granules and facilitated the transfer of samples between containers (Hillier 1999a). Afterward, the slurries were homogenized for 60 s in a McCrone mill. The spraying pressure was around 69 kPa (10 psi) and the temperature of the inner chamber was set at 155 °C. Dried granules were collected on a sheet of wax paper placed at the bottom of the drying cylinder. Product recovery was around 60–65% for sprayed samples. The spray-dried mineral mixtures were composed of round-shaped aggregates with rough surface textures and sizes ranging from 40 to 100 µm (Fig. 1).

X-ray diffraction and Rietveld analysis

X-ray diffraction patterns were recorded on a Bruker D8 diffractometer in Bragg-Brentano geometry (θ-θ goniometer) using Cu*K*α radiation generated at 40 kV and 40 mA. The instrument was operated with a 0.2 mm divergence slit, 2.5° primary and secondary Soller slits, a 2.459° detector opening, and a high-resolution Lynxeye XE-T detector. Samples were measured from 3 to 100 °2θ with a step size of 0.006 °2θ and a measuring time of 1.8 s per step. Mineral mixtures prepared conventionally were measured with rotation (30 rpm), while spray-dried mixtures were measured without rotation because of the flowability of the powder. The top-loading technique was used for sample transfer into 25 mm plastic sample holders.

Rietveld refinements of PXRD data were performed in BGMN with Profex v.5.0.1 as a graphical user interface (Doebelin and Kleeberg 2015). Profex-BGMN uses information on instrumental features such as the primary beam, secondary beam (mode and length of divergence slit, opening angle of Soller slits, axial beam mask, and sample stage), wavelength distribution of the X-ray source, instrument detector, and the contribution of phases such as crystallite size and micro strain for the configuration of peak profiles. The peak shape function can be described by the deconvolution of wavelength distribution, instrument function, and sample function (crystallite sizes and micro strain broadening). Prior to Rietveld refinement, simulation by the Monte Carlo ray-tracing algorithm was used to obtain instrument profile functions, and instrumental profile shapes were calculated at different angular steps (Bergmann et al. 1997, 1998; Doebelin and Kleeberg 2015). Instrument parameters were set and remained unchanged during Rietveld analyses while sample functions were refined. The degree of polynomial was defined for background refinement (RU = 10 or 11) and the upper and lower limits were defined (if necessary) for each parameter present in a structure model. These parameter limits were either fixed as predefined in structure models or modified to improve the stability of refinement and the convergence of refined parameters. Statistical parameters (R_{wp}, R_{exp}, and "goodness of fit," GOF) were used to evaluate the quality of refinements. GOF equals R_{wp} divided by R_{exp}, where R_{wp} represents the weighted residual square sum assessing the difference between measured and calculated diffractograms, while R_{exp} is the lowest obtainable value of R_{wp} (Doebelin and Kleeberg 2015).

Profex-BGMN is well suited for our samples because it is able to handle structure models for stacking disordered clay minerals such as illite-smectite and kaolinite or turbostratically disordered smectite (Ufer et al. 2004, 2008, 2012b, 2015). Turbostratic disorder of interlayered materials, described as a "random rotation and/or translation of individual layers relative to each other" (Ufer et al. 2004, 2008), yields irregular, asymmetric non-basal reflections and peak shapes that cause problems during refinement with standard models and thus QPA if not adequately accounted for. In addition, the mass fractions of amorphous and individual crystalline components can be directly estimated with Profex-BGMN if the mass fraction of an internal standard is fixed before starting the refinement. We generally used structural input models of ordered phases provided in the Profex-BGMN structure file library. Disordered structure models for illite-smectite, kaolinite, and smectite were taken from the literature (Ufer et al. 2008, 2012b, 2015). Powder XRD patterns were refined between 5 and 80 °2θ. By applying the predefined upper and lower limits of parameters as given in structure models, we refined lattice constants, phase fractions, and preferred orientation by applying symmetrized harmonics (Bergmann et al. 2001) of the orders zero to six, micro strain, and isotropic line broadening, while the zero point, sample displacement, and background of powder patterns were refined as non-structural parameters. Occupation factors of cations in models remained unchanged during refinements. Refinement of preferred orientation was ignored for all spray-dried samples (order set at zero) to reveal the effect of spray drying on preferred orientation. Similarly, mineral phases present in trace amounts (<1 wt%) in illite-smectite, kaolinite, and smectite-rich bentonite (Table 1) were ignored during Rietveld analysis of mineral mixtures.

Scanning electron microscopy

For the determination of particle size and morphology of mineral mixtures, samples were dispersed on an adhesive carbon disk, sputtered with Au, and analyzed by a JEOL JSM-7610FPlus field emission scanning electron microscope to obtain secondary electron images. The probe current was set between 10 and 20 pA at an accelerating voltage of 5 kV, and the working distance ranged from 2 to 3 mm.

X-ray fluorescence spectrometry

The chemical composition of mineral mixtures was analyzed by wavelength-dispersive XRF spectrometry using a PANalytical Zetium spectrometer. Approximately 1 g of oven-dried (105 °C) mineral mixtures was weighed to the fourth decimal place, then heated at 1030 °C for 10 min, cooled in a desiccator, and reweighed to determine the LOI. Elements or compounds lost during heating include organics, CO_2, SO_2, Cl, and structural water. The remaining ignited samples were mixed with 5.0 g lithium metaborate (Spectroflux 100A, Alfa Aesar)

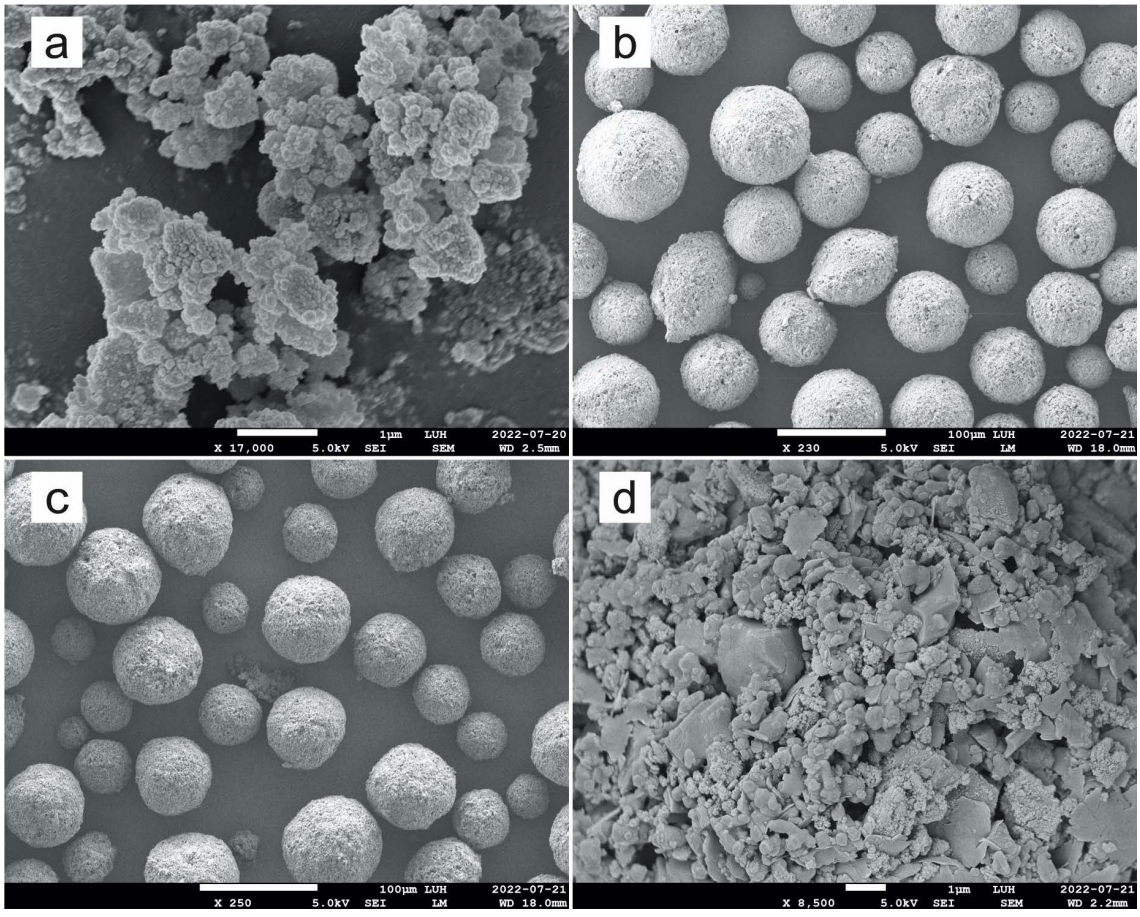

Figure 1. Scanning electron microscopy images of iXAMs used in this study [1:1 weight mixture of ferrihydrite and opal-A] before (**a**) and after (**b**) spray drying, (**c**) spray-dried mineral mixture B with 40 wt% iXAMs, and (**d**) particle surface morphology of the spray-dried sample of mineral mixture B. Scale bars in **a** and **d** are 1 µm and those in **b** and **c** 100 µm.

and 25 mg of lithium bromide and fused at 1200 °C for 20 min in a Herzog HAG 12/1500 fusion digestion unit. The obtained glass disks were analyzed by XRF spectrometry. Instrument calibrations were validated by analysis of reference materials and in-house standards, as well as 130 certified reference materials were used for data correction procedures.

Thermogravimetry and DSC analyses

Ferrihydrite, opal-A, and their 1:1 mixture were analyzed by thermogravimetry (TG) and differential scanning calorimetry (DSC). TG-DSC measurements were carried out using a Setsys Evolution 1750 instrument (SETARAM). Samples were heated from 25 to 1000 °C at a rate of 5 °C/min under a flow of N_2 set at 30 mL/min.

Data analysis

Statistical analyses were performed in SigmaPlot v.15 (Inpixon GmbH). Data were evaluated by test statistics and linear regression analyses. Significant differences between variable groups were evaluated by Student's and Welch's t-tests, Mann-Whitney rank sum test, and one-way analysis of variance (ANOVA) with subsequent post-hoc tests for multiple comparisons (Holm-Sidak method and Tukey test). Normality of data and homogeneity of variances were analyzed using the Shapiro-Wilk and Brown-Forsythe tests, respectively. Differences were considered significant at $P < 0.05$. The accuracy ("true value") of iXAM content and composition was evaluated by comparing nominal and Rietveld-based values, while the precision of iXAM quantification was determined by repeated (N = 5) sample preparation (mixing of mineral mixture with 10 wt% iXAMs and 30 wt% corundum, followed by convention sample preparation and spray drying) and Rietveld analysis of selected mineral mixtures. Detection and quantification limits of iXAMs were evaluated following DIN 32645 as described in Funk et al. (2005). The quantification limit was calculated with a maximum admissible error of the analytical result of 10% (*k*-value).

Results

In the following, we first detail aspects of sample preparation and general Rietveld fit quality. We then address accuracy, precision, and limits of detection and quantification of the Rietveld method for iXAM quantification. Afterward, we examine the accuracy of the Rietveld method for crystalline mineral components in mineral mixtures before applying the balance sheet method to quantify the chemical composition of iXAMs in mineral mixtures and evaluate the accuracy of this approach.

Sample preparation and Rietveld fit quality

Figure 2 displays diffractograms of conventionally prepared ferrihydrite and opal-A, and their 1:1 mixture prepared conventionally and by spray drying. Apparently, spray drying of iXAMs at 155 °C did not alter their diffractogram, documenting the absence of iXAM transformations into more crystalline phases during spray drying. Spray drying also effectively eliminated the effect of the preferred orientation for clay minerals. Figure 3

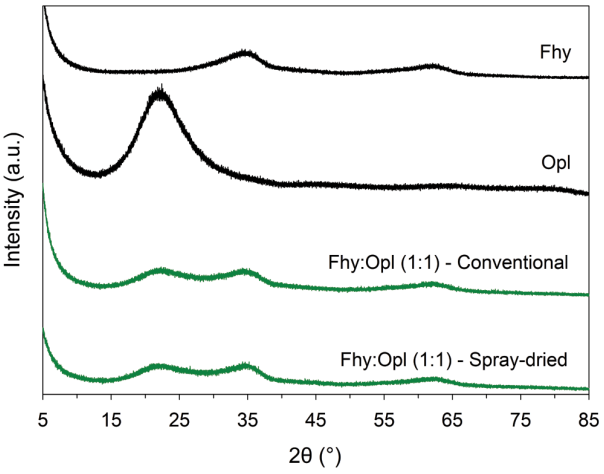

Figure 2. PXRD patterns of conventionally prepared ferrihydrite (Fhy), opal-A (Opl), and their 1:1 (w/w) mixture as well as the spray-dried mixture of ferrihydrite and opal-A. (Color online.)

compares diffractograms of mineral mixtures C and D prepared conventionally and by spray drying. Mixture C represented the least complex mineral mixture, while mixture D was the most complex, as it contained the highest numbers of minerals and disordered clay minerals. For chlorite in both mixtures, 00*l* reflections at 6.17, 12.4, 18.6, and 24.9 °2θ, when scaled to the quartz 1–10 reflection at 20.8 °2θ, were strongly reduced after spray drying. Similarly, the broad peak of the disordered illite-smectite at 7.5–9.2 °2θ was markedly reduced in the spray-dried mixtures (Fig. 3).

Figure 4 shows an example of Rietveld fits for mineral mixture B containing 40 wt% iXAMs and both sample preparation methods. The figure illustrates that peak intensities were correctly matched in both cases. Generally, significantly smaller GOF values ($P < 0.001$) were recorded for conventionally prepared mixtures (Online Materials[1] Tables S1 and S2). For all analyzed mineral mixtures with or without iXAMs that were conventionally prepared, GOF values ranged from 1.23 to 1.84 (mean = 1.44), while GOF values for spray-dried mixtures ranged from 1.44 to 1.90 (mean = 1.63). Likewise, for individual mineral mixtures A–D with 0–70 wt% iXAMs, the conventional sample preparation always resulted in significantly lower GOF values ($P \leq 0.028$) than spray drying (Online Materials[1] Table S2). We found that the addition of iXAMs to mineral mixtures resulted in lower GOF values compared to the original mineral mixtures and slightly higher GOF values at the upper end (>50 wt%) of nominal iXAM contents for all mineral mixtures and sample preparation methods (Online Materials[1] Table S1). The reason for the higher GOF values for the spray-dried compared to the conventionally prepared mineral mixtures is that correction for preferred orientation by spherical harmonics was not applied during Rietveld refinements, and thus, fewer parameters were refined. Comparisons of GOF values for different mineral mixtures revealed that sample composition had a significant effect on Rietveld fit quality only for the conventionally prepared mixtures caused by mixture B (Online Materials[1] Table S2).

Quantification of iXAMs

We tested the accuracy of iXAM quantification in mineral mixtures depending on the complexity of crystalline mineral assemblages for both sample preparation methods. The abundances of iXAMs in mineral mixtures determined by the Rietveld method are illustrated in Figure 5, and Table 3 summarizes values

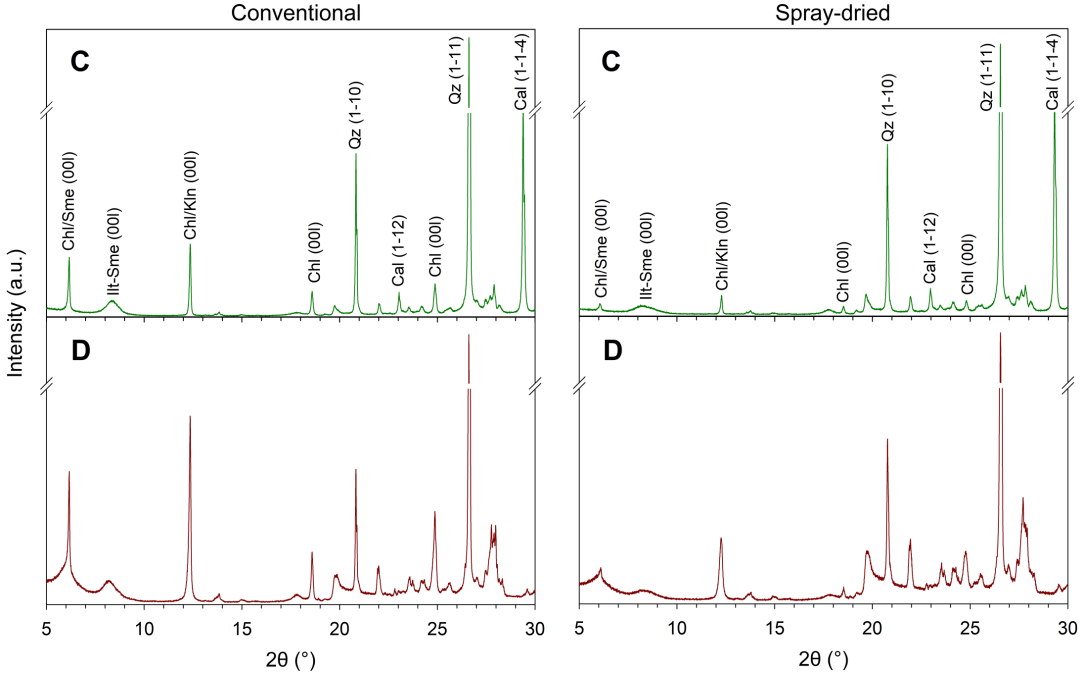

Figure 3. PXRD patterns of mineral mixtures C (least complexity) and D (highest complexity) after conventional sample preparation and spray drying. Cal = calcite; Chl = chlorite; Ilt-Sme = illite-smectite; Kln = kaolinite; Qz = quartz. (Color online.)

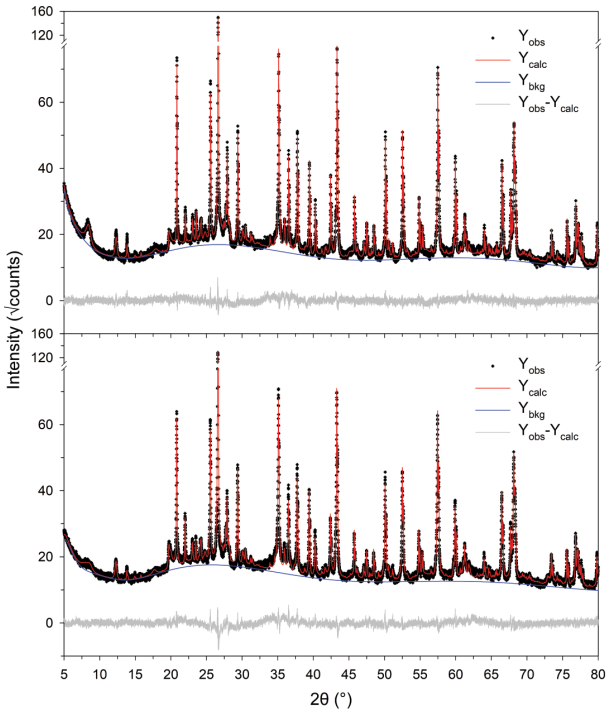

Figure 4. Rietveld refinements of mineral mixture B containing 40 wt%. iXAMs after conventional sample preparation (**top**) and spray drying (**bottom**). (Color online.)

of iXAM contents along with estimated standard deviations as well as absolute and relative quantification errors. Linear relationships between nominal and Rietveld-derived iXAM contents with R^2 values >0.99 and regression slopes of 0.94–0.98 for the conventionally prepared mixtures and of 0.95–0.99 for the spray-dried mixtures (Fig. 5) confirm a high degree of accuracy in iXAM quantification for both sample preparation methods and different mineral assemblages. We found no significant difference between regression slopes for both sample preparation methods (P = 0.855). QPA results obtained by Rietveld refinements indicated that all starting mineral mixtures with 0 wt% nominal iXAM contents contained an intrinsic amount of amorphous materials and amorphicity induced during sample preparation by milling and mixing of 1.18–3.92 wt% (Fig. 5; Online Materials[1] Table S1). This intrinsic amorphous part also includes phases that are contained in trace amounts (i.e., not quantifiable by Rietveld) and the amorphous portion of crystalline phases.

Figure 6 illustrates the frequency distribution of the deviation between nominal and Rietveld-determined iXAM contents in all mineral mixtures for both sample preparation methods after correction for the intrinsic and milling/mixing induced amorphicity of crystalline phases. This data shows that absolute errors of iXAM determination were within ±2 wt% for both sample preparation methods with no gross outliers. The error distributions were non-Gaussian and suggested a slight tendency of iXAM overestimation, which was less pronounced for the spray-dried mineral mixtures. Nonetheless, neither method led to a significant difference in absolute quantification errors

Table 3. Comparison between nominal and Rietveld-derived iXAM contents (wt%) for mineral mixtures A–D after conventional sample preparation and spray drying with estimated standard deviations (e.s.d.) as well as absolute (wt%) and relative (%) quantification errors

	Conventional				Spray-dried			
Nominal	Rietveld	e.s.d.	Abs. error	Rel. error	Rietveld	e.s.d.	Abs. error	Rel. error
Mixture A								
10	11.33	0.27	1.33	13.3	9.43	0.23	−0.57	5.71
20	19.40	0.29	−0.60	3.02	21.11	0.23	1.11	5.54
30	30.75	0.27	0.75	2.51	29.65	0.22	−0.35	1.18
40	38.50	0.29	−1.50	3.74	40.59	0.22	0.59	1.47
50	48.57	0.26	−1.43	2.86	48.94	0.23	−1.07	2.13
60	58.03	0.26	−1.97	3.29	58.01	0.20	−1.99	3.31
70	68.17	0.22	−1.83	2.62	68.50	0.17	−1.50	2.14
Mixture B								
10	10.81	0.26	0.81	8.14	10.37	0.22	0.37	3.72
20	20.17	0.25	0.17	0.84	20.72	0.23	0.72	3.62
30	31.97	0.25	1.97	6.57	30.74	0.22	0.74	2.45
40	40.13	0.25	0.13	0.31	40.90	0.21	0.90	2.24
50	50.79	0.24	0.79	1.58	51.73	0.22	1.73	3.46
60	61.09	0.20	1.09	1.82	61.71	0.20	1.71	2.85
70	69.63	0.21	0.37	0.53	70.60	0.17	0.60	0.86
Mixture C								
10	9.91	0.27	−0.09	0.87	10.23	0.23	0.23	2.33
20	21.83	0.26	1.83	9.13	20.96	0.24	0.96	4.78
30	30.63	0.26	0.63	2.10	29.49	0.22	−0.51	1.70
40	41.89	0.23	1.89	4.73	41.14	0.20	1.14	2.85
50	51.26	0.22	1.77	2.51	51.80	0.22	1.80	3.59
60	61.77	0.22	1.77	2.95	61.80	0.19	1.80	3.00
70	69.51	0.22	−0.49	0.70	69.32	0.20	−0.68	0.97
Mixture D								
10	10.05	0.32	0.04	0.45	9.85	0.23	−0.15	1.52
20	18.80	0.28	−1.20	6.00	20.09	0.25	0.09	0.43
30	28.84	0.30	−1.17	3.88	31.15	0.22	1.15	3.85
40	38.49	0.27	−1.51	3.78	39.10	0.23	−0.90	2.24
50	49.54	0.26	−0.47	0.93	48.65	0.22	−1.35	2.70
60	61.24	0.23	1.24	2.07	58.46	0.20	−1.54	2.57
70	69.62	0.22	−0.38	0.55	69.49	0.19	−0.51	0.73

Note: Rietveld-derived iXAM contents were corrected for the initial amorphous content of mineral mixtures.

(Mann-Whitney rank sum test, P = 0.922, N = 28). Relative errors of Rietveld-determined iXAM contents ranged from 0.31 to 13.3% and increased with decreasing iXAM content (Fig. 7). Conventionally prepared mineral mixtures resulted in a larger spread of relative errors for nominal iXAM contents <50 wt% when compared to the spray-dried mineral mixtures (Fig. 7). Means and standard deviations (2σ, equivalent to the 95% confidence level) of iXAM quantification errors for each mineral mixture are listed in Table 4. Statistical tests for individual mineral mixtures (A–D) showed that there were no significant differences in absolute iXAM quantification errors between both sample preparation methods. Combined means ±2σ of absolute quantification errors for the four mineral mixtures were 0.14 ± 2.47 and 0.16 ± 2.21 wt% for the conventional and spray drying sample preparation method, respectively. Consequently, absolute errors in iXAM quantification appear to be indifferent for both sample preparation methods. The total absolute quantification error (mean ±2σ) calculated from all mineral mixtures and sample preparation methods was 0.15 ± 2.32 wt% (N = 56).

Figure 8 shows the results of iXAM quantification based on repetitive sample preparation and analysis (N = 5) of mineral mixtures B–D amended with 10 wt% iXAMs. Absolute errors in iXAMs quantification ranged from –1.69 to 1.11 wt% for the conventionally prepared mixtures (mean ±2σ = –0.21 ± 1.61 wt%)

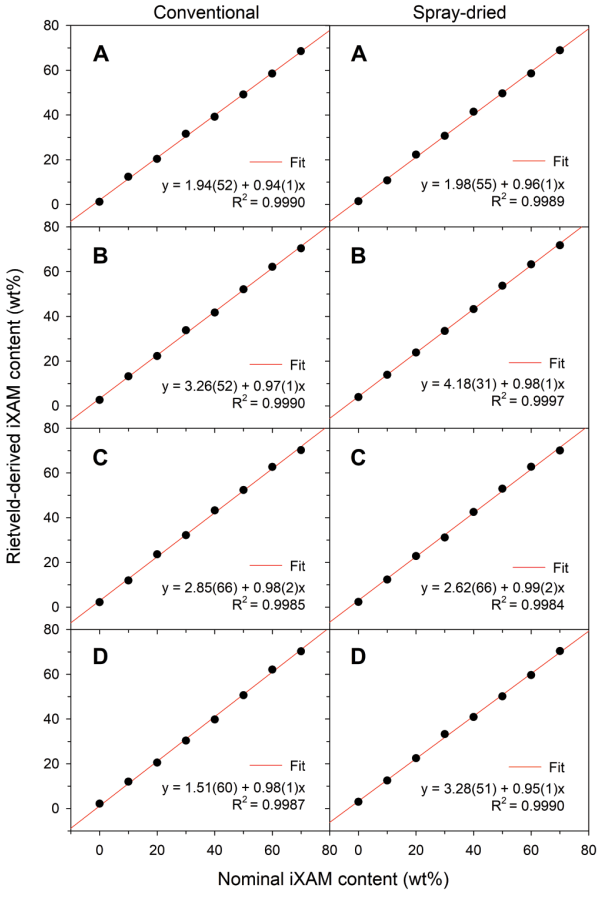

FIGURE 5. Linear relationships between nominal and Rietveld-derived iXAM contents of mineral mixtures A–D amended with 10–70 wt% iXAMs after conventional sample preparation and spray drying (data uncorrected for the initial amorphous content of mineral mixtures). (Color online.)

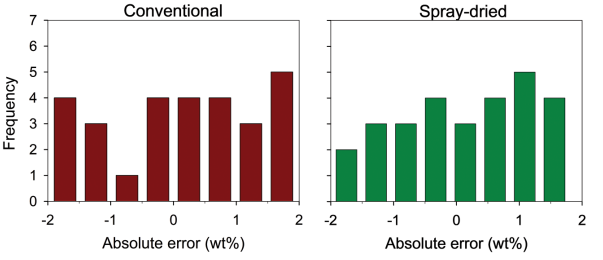

FIGURE 6. Frequency distribution of absolute iXAM quantification errors for mineral mixtures A–D amended with 10–70 wt% iXAMs after conventional sample preparation and spray drying (data corrected for the initial amorphous content of mineral mixtures). (Color online.)

and from –1.08 to 1.24 wt% for the spray-dried mixtures (mean ±2σ = 0.16 ± 1.49 wt%). These numbers imply that the spray drying resulted in more precise iXAM results when compared to the conventional sample preparation method. However, we found no significant effect of sample preparation method on average quantification errors of the same mineral mixtures (Fig. 8). We also found that mineral assemblage complexity only produced

TABLE 4. Absolute (wt%) and relative errors (%) of iXAM quantification by mineral mixture after conventional sample preparation and spray drying

		Conventional		Spray-dried	
Mixture		Abs. error	Rel. error	Abs. error	Rel. error
A	Mean	–0.75	4.48	–0.54	3.07
	2σ	2.61	7.81	2.21	3.75
B	Mean	0.76	2.83	0.97	2.75
	2σ	1.29	6.34	1.08	2.02
C	Mean	1.04	3.28	0.68	2.75
	2σ	2.03	5.83	2.04	2.50
D	Mean	–0.49	2.52	–0.46	2.01
	2σ	1.88	4.20	1.85	2.39
Total[a]	Mean	0.14	3.28	0.16	2.64
	2σ	2.47	6.02	2.21	2.70
General[b]	Mean	0.15	2.96		
	2σ	2.32	4.67		

[a] For all mixtures of each sample preparation method.
[b] For all mixtures and both sample preparation methods.

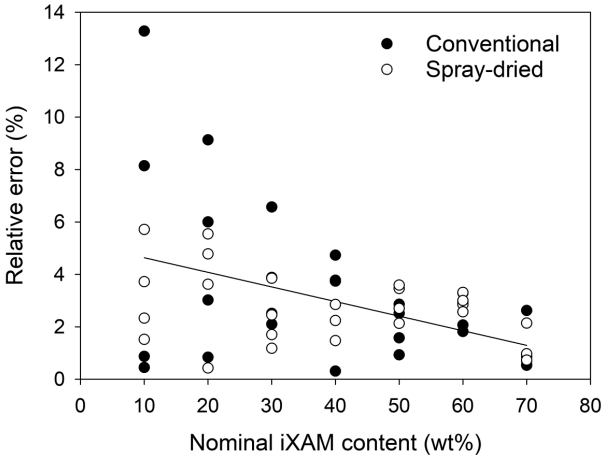

FIGURE 7. Relative iXAM quantification errors for mineral mixtures A–D amended with 10–70 wt% iXAMs after conventional sample preparation and spray drying (data corrected for the initial amorphous content of mineral mixtures). The regression line applies to all data.

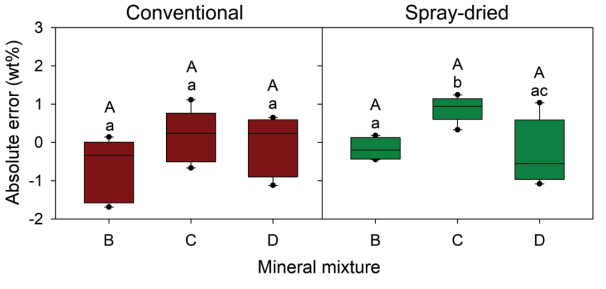

FIGURE 8. Boxplots illustrating the precision of iXAM quantification for mineral mixtures B–D amended with 10 wt% iXAMs (N = 5 for each mixture) after conventional sample preparation and spray drying (data corrected for the initial amorphous content of mineral mixtures). The boxes contain 50% of the data (interquartile range, IQR). The middle line represents the median (50th percentile). Whiskers include data within 1.5 × IQR. Different uppercase letters indicate significant differences between each mineral mixture prepared either conventionally or by spray drying, and different lowercase letters indicate significant differences between all mineral mixtures for each sample preparation method. (Color online.)

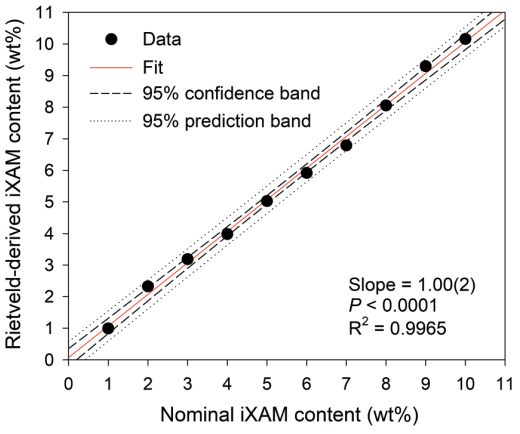

FIGURE 9. Linear calibration function of nominal vs. Rietveld-derived iXAM contents of spray-dried mineral mixture B amended with 1–10 wt% iXAMs (data corrected for the initial amorphous content of the mineral mixture). (Color online.)

significant differences in iXAM quantification errors for the spray-dried mixtures (Fig. 8). Figure 8 also shows that mineral mixture D having the highest complexity produced the largest deviations from nominal iXAM contents for the spray-dried mixtures. Combining all data of Figure 8, the average precision of iXAM quantification ±2σ was –0.03 ± 1.57 wt% (N = 30).

To determine limits of iXAM detection and quantification following DIN 32645, we amended mineral mixture B with 1–10 wt% iXAMs in 10 concentration steps (Fig. 9). A regression slope of 1.00(2) and data points falling into the 95% prediction band testify that iXAMs can be accurately determined by the Rietveld method. From the linear calibration function of nominal against Rietveld-derived iXAM contents—corrected for the amorphicity of the initial mineral mixture as constant factor—we obtained iXAM detection and quantification limits of 0.8 and 4.0 wt%, respectively. Absolute and relative method standard deviations were calculated to be 0.18 wt% and 3.26%, respectively.

Chemical composition of iXAMs

For the accurate assessment of the chemical composition of iXAMs by the balancing of oxide masses obtained from PXRD and XRF data, the correct quantification of crystalline minerals in a given sample by the Rietveld method is a key prerequisite. Nominal vs. Rietveld-determined contents of crystalline minerals are exemplarily shown in Figures 10 and 11 for mineral mixtures C (lowest complexity) and D (highest complexity), respectively. Online Materials[1] Figures S1 and S2 show analogous data for mineral mixtures A and B, and Online Materials[1] Tables S1 and S3 summarize quantified mineral contents for all mineral mixtures and their errors. Generally, both sample preparation methods produced statistically similar absolute quantification errors for all crystalline minerals (quartz, feldspars, calcite, illite-smectite, chlorite, kaolinite, and smectite). The spray drying method occasionally proved to be more accurate in the quantification of feldspars than the conventional sample preparation method (Online Materials[1] Table S3). In general, however, we found no significant differences in feldspar quantification errors between mineral mixtures using either sample preparation method (Online Materials[1] Table S4). Both sample preparation methods resulted in an overestimation of disordered illite-smectite, with a tendency toward greater errors in spray-dried compared to conventionally prepared mineral mixtures (Fig. 11; Online Materials[1] Figs. S1 and S2).

Figure 12 shows histograms of quantification errors for all crystalline minerals and both sample preparation methods. As opposed to absolute quantification errors of iXAMs (Fig. 6), absolute quantification errors of crystalline minerals were normally distributed. Absolute quantification errors varied from –6.1 to 4.3 wt% for the conventionally prepared mineral mixtures (mean ± 2σ = –0.25 ± 2.94 wt%, N = 192) and from –3.8 to 4.1 wt% (mean ± 2σ = –0.31 ± 2.78 wt%, N = 192) for the spray-dried mixtures. The total mass bias of crystalline minerals determined for all iXAM levels ranged from 3.6 wt% in mixture C to 12.7 wt% (mean ± 2σ = 6.67 ± 4.96 wt%) in mixture A for the conventional sample preparation and from 2.5 wt% in mixture C to 12.2 wt% in mixture D for the spray-dried samples (mean ± 2σ = 6.62 ± 4.68 wt%). Generally, this indicates that there was only a small difference in the quantification of crystalline minerals between both sample preparation methods and that the total mass bias increased with increasing sample complexity.

Because the quantification of clay minerals is critical to arrive at an accurate chemical composition of soil iXAMs, we analyzed their Rietveld quantifi-

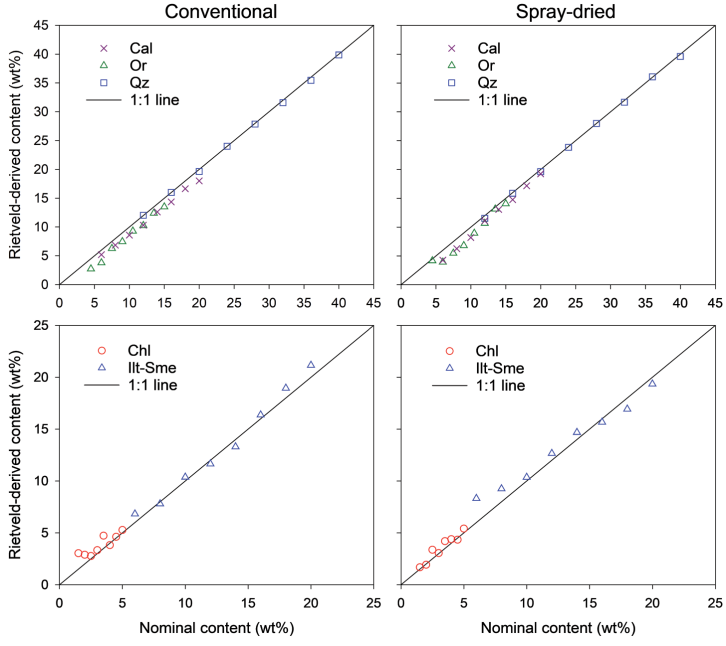

FIGURE 10. Plots of nominal vs. Rietveld-derived contents of crystalline non-clay and clay minerals in mineral mixture C amended with 0–70 wt% iXAMs after conventional sample preparation and spray drying. Cal = calcite; Chl = chlorite; Ilt-Sme = illite-smectite; Or = orthoclase; Qz = quartz. (Color online.)

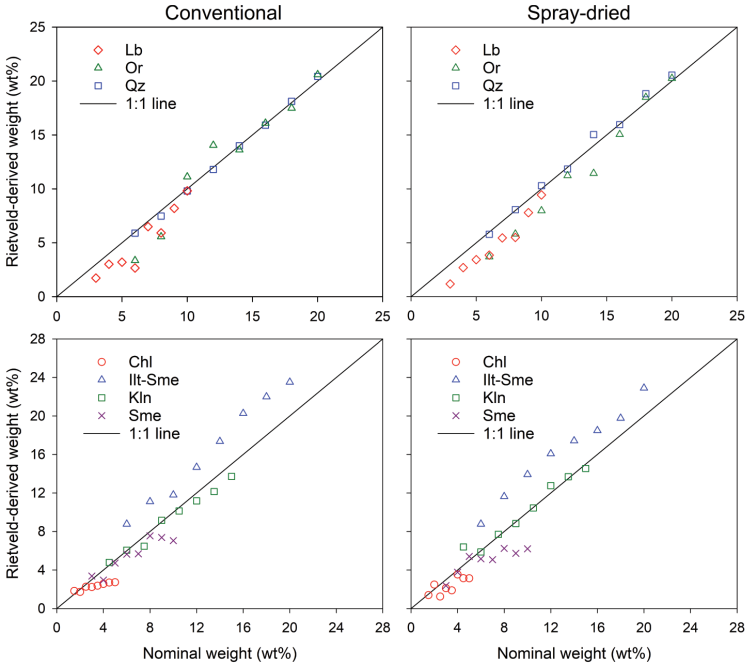

FIGURE 11. Plots of nominal vs. Rietveld-derived contents of crystalline non-clay and clay minerals in mineral mixture D amended with 0–70 wt% iXAMs after conventional sample preparation and spray drying. Chl = chlorite; Ilt-Sme = illite-smectite; Kln = kaolinite; Lb = labradorite; Or = orthoclase; Qz = quartz; Sme = smectite. (Color online.)

cation errors in detail (Online Materials[1] Tables S5–S7). For the sum of clay minerals (chlorite, illite-smectite, kaolinite, and smectite), we found no significant effects of the sample preparation method and sample composition on their absolute quantification errors (Online Materials[1] Table S5). However, the complexity of mineral assemblages significantly affected Rietveld quantification errors for chlorite and illite-smectite (but not kaolinite), irrespective of sample preparation method (Online Materials[1] Table S6).

Figure 13 illustrates the comparison between XRF- and Rietveld-derived oxide contents for all initial mineral mixtures A–D and both sample preparation methods. The chemical compositions of crystalline minerals were taken from structure models used in the Rietveld refinements. XRF-derived chemical compositions of all initial mineral mixtures A–D and iXAM-amended mineral mixtures B–D are summarized in Online Materials[1] Tables S8 and S9, respectively. For all initial mineral mixtures and both sample preparation methods, SiO_2 and Fe_2O_3 contents derived from XRF spectrometry and Rietveld analysis always showed a good correspondence (±3 wt%) (Fig. 13; Online Materials[1] Table S8). There was also a good agreement (±2 wt%) between Al_2O_3, Na_2O, K_2O, CaO, and MgO contents. XRF spectrometry results (Online Materials[1] Tables S8 and S9) showed that TiO_2 (≥0.1 wt%.) was present in mineral mixtures A, B, and D because of trace amounts of anatase in kaolinite, which remained undetected by PXRD. The highest amount of TiO_2 was therefore recorded for mixture D having the highest kaolinite content (Table 2). Generally, deviations between oxide contents determined by XRF spectrometry and Rietveld analysis became more apparent for oxide concentrations <4 wt% (Fig. 13).

Based on XRF and Rietveld data, we employed the balance sheet method to calculate the chemical composition of iXAMs in mineral mixtures prepared conventionally and by spray drying (Online Materials[1] Table S10). A detailed breakdown of the oxide mass-balance calculation is exemplified in Table 5 for the spray-dried mixture B containing 40 wt% iXAMs. Data in Table 5 illustrate that the balance sheet method yielded an accurate iXAM chemical composition in terms of nominal SiO_2 and Fe_2O_3 contents (absolute errors <1.4 wt%), but a larger discrepancy between nominal and XRF/Rietveld derived LOI of iXAMs (absolute and relative error = 1.39 wt% and 23%, respectively). The total oxide plus LOI content of 43.1 wt% determined by the balance sheet method for iXAMs in this sample was identical within error to the iXAM content quantified by Rietveld analysis (43.3 wt%; Table 5). The mass balance approach also resulted in the assignment of other oxides than SiO_2 and Fe_2O_3 (e.g., Al_2O_3, Na_2O, and CaO) to the iXAM fraction of all analyzed mixtures (Table 5; Online Materials[1] Table S10). However, their summed quantities generally remained below 3 wt% (Online Materials[1] Table S11).

Figure 14 displays the mass-balance-derived chemical composition of iXAMs in terms of SiO_2, Fe_2O_3, and LOI contents as major constituents of the iXAMs used, along with their relative errors for mineral mixtures B–D and both sample preparation methods. In terms of SiO_2, Fe_2O_3, and LOI contents, both sample preparation methods resulted in largely equivalent results (Online Materials[1] Table S10). For all samples analyzed, deviations of quantified oxide contents from their nominal values ranged from –2.64 to 1.51 wt% for SiO_2 (mean ± 2σ = 0.01 ± 2.39 wt%) and

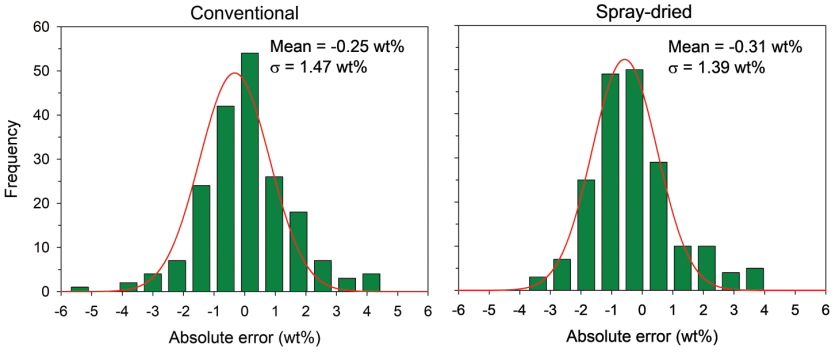

FIGURE 12. Frequency distribution of absolute quantification errors for crystalline mineral phases in mineral mixtures A–D amended with 0–70 wt% iXAMs after conventional sample preparation and spray drying. The red lines show fits of Gaussian functions and are meant to guide the eye. (Color online.)

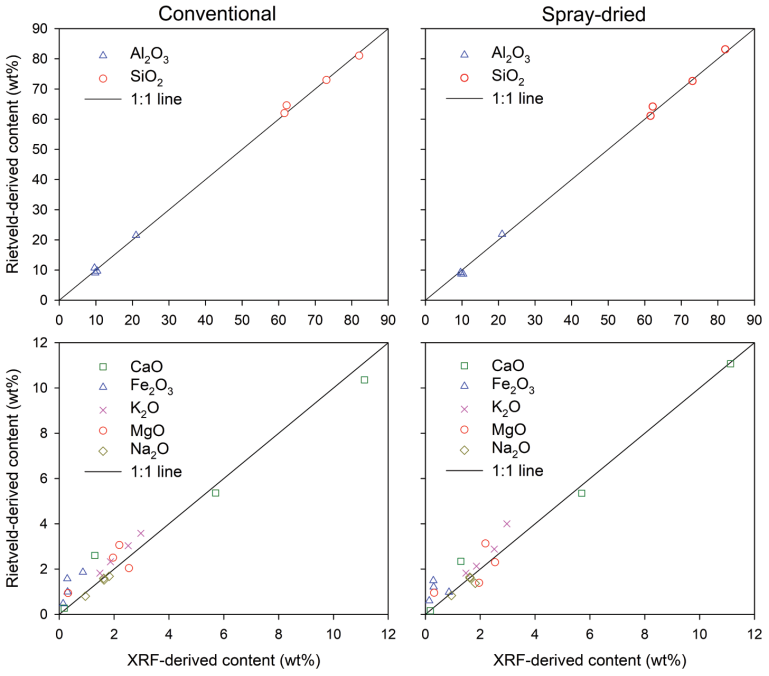

FIGURE 13. Comparison of XRF- and Rietveld-derived chemical compositions of initial mineral mixtures A–D after conventional sample preparation and spray drying. (Color online.)

from –1.53 to 0.39 wt% for Fe_2O_3 (mean ± 2σ = –0.40 ± 0.96 wt%) (Online Materials[1] Table S12). Relative errors associated with these numbers were 0.07–54.7% for SiO_2 (mean ± 2σ = 9.39 ± 23.4%) and 0.02–35.6% for Fe_2O_3 (mean ± 2σ = 4.26 ± 12.20%). The relative errors of the major two oxides were mostly within an acceptable error limit of ±10% but can be much higher in complex mineral mixtures, especially at low iXAM contents (Fig. 14).

The LOI comprising mainly adsorbed H_2O and structural H_2O/OH^- was an important constituent of the iXAMs used in this study. XRF analysis of the 1:1 ferrihydrite-opal mixture delivered a LOI of 15.3 wt%, which is close to the 14.0% weight loss of the mixture upon heating up to 1000 °C during TG analysis (Online Materials[1] Fig. S3). The LOI determined for iXAMs in all mineral mixtures deviated between 0.14 and 5.69 wt% from nominal values (mean ± 2σ = 2.19 ± 2.78 wt%), and relative errors ranged from 1.30 to 371% (mean ± 2σ = 67.2 ± 171%) (Fig. 14). Pooling all samples for each sample preparation method, we obtained excellent linear relationships with an R^2 > 0.99 between the nominal and mass-balanced derived sum of SiO_2, Fe_2O_3, and LOI contents of iXAMs in the mineral mixtures (Fig. 15). Regression slopes were indifferent for both sample preparation methods and slightly lower than unity. The latter was caused by an overestimation of the LOI for iXAMs, particularly at the lower end of iXAM contents (Fig. 14; Online Materials[1] Table S12). There was no significant difference in absolute quantification errors of summed SiO_2, Fe_2O_3, and LOI contents between both sample preparation methods.

DISCUSSION

We found a good agreement between observed and Rietveld calculated PXRD patterns for both sample preparation methods. The improved Rietveld fit quality observed after iXAM addition to mineral mixtures (Online Materials[1] Table S1) likely originates from a reduced preferred orientation of crystalline minerals (Tsukimura 1997). Deteriorated fits at the upper end of iXAM contents (Online Materials[1] Table S1) were probably caused by increased background levels of the refined powder patterns, which decreased the integrated intensities and thus phase fractions associated with crystalline minerals (Gualtieri 2000). In contrast to previous studies (Chung 1974; Gualtieri 2000; Hillier 2000; Monecke et al. 2001; Chipera and Bish 2002, 2013), the quality of our Rietveld refinements was hardly affected by disordered clay minerals containing illite-smectite, kaolinite, and smectite, because suitable structure models accounting for stacking disorder (Ufer et al. 2004, 2008, 2012b, 2015) were readily available. However, we observed that the overestimation of disordered illite-smectite led to the underestimation of feldspars, but this did not affect the accuracy of quartz and calcite contents (Figs. 11 and Online Materials[1] Fig. S1; cp. Table 2 and Online Materials[1] Table S1). Increasing overlap of peaks originating from amorphous materials and disordered clay minerals is likely to cause increasing deviations in Rietveld-derived mineral contents from their true values, especially when clay minerals (and feldspars) reach XRD detection and quantification limits

TABLE 5. Example balance sheet calculation for the assignment of oxides (X-ray fluorescence data given in parentheses) to the iXAM fraction of spray-dried mineral mixture B containing 40 wt% iXAMs

Mineral[a]	Oxides										
	SiO_2 (60.61)	TiO_2 (0.08)	Al_2O_3 (6.24)	Fe_2O_3 (17.35)	MgO (0.20)	CaO (3.51)	Na_2O (1.01)	K_2O (1.11)	LOI[b] (9.66)	Total (99.77)	Rietveld[c]
Ab	3.20	–	1.02	–	–	–	0.58	–	–		4.78(16)
Cal	–	–	–	–	–	2.74	–	–	2.14		4.87(3)
Or	3.18	–	1.02	–	–	0.09	0.27	0.38	–		4.97(12)
Qz	28.52	–	–	–	–	–	–	–	–		28.52(8)
Ilt-Sme	6.31	–	2.52	0.24	0.71	–	–	1.10	–		10.88(13)
Kln	1.50	–	1.27	–	–	–	–	–	–		2.77(5)
iXAMs[d]	17.90	0.08	0.41	17.11	–0.51	0.69	0.17	–0.36	7.52	43.12	43.25(21)

Note: All values are given in wt%. [a] Mineral abbreviations: Ab = albite; Cal = calcite; Ilt-Sme = illite-smectite; Kln = kaolinite; Or = orthoclase; Qz = quartz.
[b] Loss on ignition.
[c] Standard deviations (σ) in parentheses apply to the last digit.
[d] Nominal oxide and LOI contents of iXAMs in mineral mixture (wt%): SiO_2 = 16.51, Fe_2O_3 = 17.22, and LOI = 6.13.

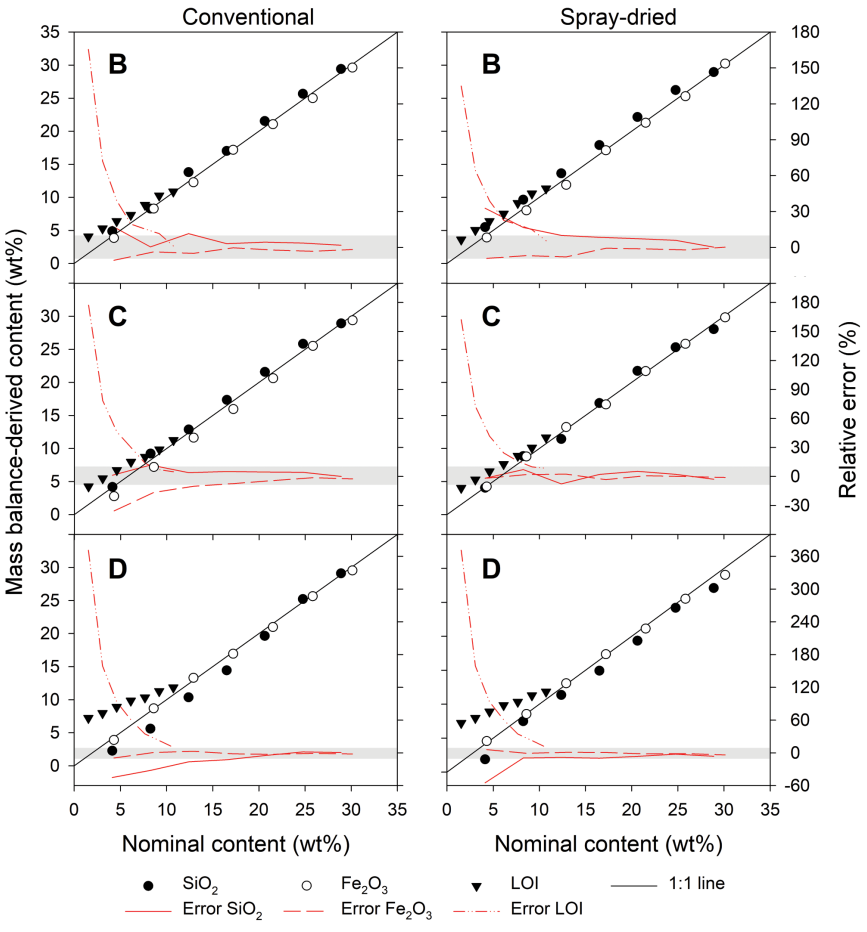

FIGURE 14. Comparison of nominal and mass balance-derived iXAM contents of SiO_2, Fe_2O_3, and LOI and their relative errors for mineral mixtures B–D amended with 10–70 wt% iXAMs after conventional sample preparation and spray drying. Nominal oxide contents were determined by XRF spectrometry. Gray shaded areas mark the ±10% error margin. (Color online.)

(Hillier 1999b). Despite the incorporation of mathematical algorithms for preferred orientation in many Rietveld software packages, reliable results for crystalline minerals cannot always be assured (McCusker et al. 1999). Our results document that the spherical harmonics algorithm provided by Bergmann et al. (2001) in Profex-BGMN was able to provide a very good agreement between nominal and Rietveld-derived contents of crystalline mineral phases (Figs. 10 and 11) and iXAMs (Fig. 5) in mineral mixtures. Therefore, we found no significant difference between the conventional and spray-drying sample preparation methods for the quantification of crystalline minerals and iXAMs in mineral mixtures using Rietveld analysis. Spray drying slightly improved the precision of iXAM quantification and is therefore preferable to the conventional sample preparation method when accounting for the effects of the preferred orientation of crystalline minerals (Bish and Reynolds 1989; Hillier 1999a, 2000). However, spray drying produced a higher precision variability as controlled by sample complexity when compared to the conventional sample preparation method (Fig. 8). Generally, QPA results from Rietveld analysis became less accurate with increasing contents of disordered clay minerals, caused by the overlap of their broad diffraction peaks with the diffuse scattering peaks of iXAMs.

So far, only few studies have provided results on the accuracy of Rietveld analyses for geological samples or mineral assemblages resembling geological or soil samples (Gualtieri 2000; Hillier 2000; Monecke et al. 2001). Previous studies showed that the accuracy achieved by Rietveld analysis is highly dependent on sample type and complexity (Bish and Post 1993; Hillier 2000; Monecke et al. 2001). With the Rietveld method, Hillier (2000) obtained an absolute error of 10.2 wt% for the amorphous fraction (glass) in an artificial sandstone mixture but achieved a better result of 1.2 wt% for the same mixture using the RIR method. Similarly, a study on a family of zeolite-rich sedimentary rock samples analyzed by the combined Rietveld-RIR method showed deviations of 0.3–1.6 wt% for glass contents ranging between zero and 20 wt% (Gualtieri 2000). At the 95% confidence level, we achieved an average accuracy of ±3 wt% for both crystalline minerals and iXAMs in mineral mixtures amended with 10–70 wt% iXAMs for both

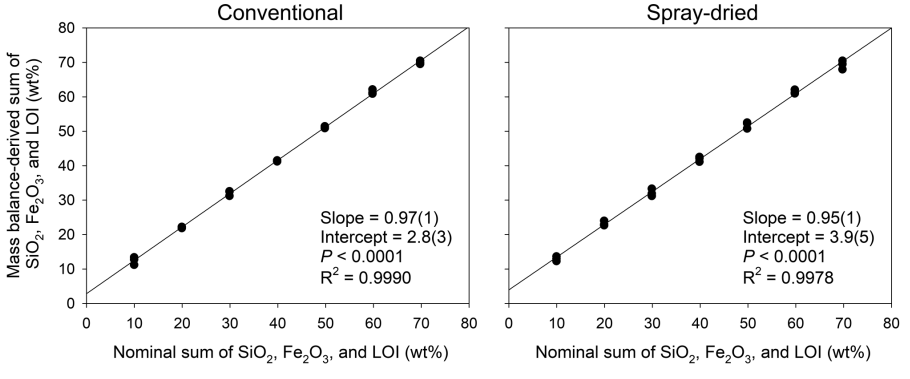

FIGURE 15. Regression of nominal and mass-balance-derived sums of SiO_2, Fe_2O_3, and LOI in iXAMs for mineral mixtures B–D amended with 10–70 wt% iXAMs after conventional sample preparation and spray drying. Nominal oxide contents were determined by XRF spectrometry.

sample preparation methods, which is identical to estimates of maximum uncertainties for crystalline minerals following QPA of PXRD data published by Hillier (2000) for the RIR method and by Gualtieri (2000) for the Rietveld-RIR method. Results of QPA of PXRD data with absolute errors within ±3 wt% or 10% relative error are generally considered "highly accurate" or "excellent" (Calvert et al. 1989; Reynolds 1989). Including both sample preparation methods, we obtained a generalized precision of iXAM quantification by the Rietveld method of ±2 wt% at the 95% confidence level and relative iXAM quantification errors <10% (except for one case; Fig. 7). Our data thus imply that iXAMs in mineral mixtures can be accurately and precisely determined by Rietveld analysis of PXRD patterns provided there are suitable crystallographic models for all crystalline minerals in a given sample. For this, the internal standard quantity of 30 wt% proposed by Jones et al. (2000) proved appropriate for the wide range of amorphous contents in our mineral mixtures.

Data on iXAM detection and quantification limits are not available in the literature. Our results indicate that soil iXAMs may not be accurately quantified by Rietveld analysis when present at concentrations of less than about 4 wt% but are already detectable at a 1 wt% level. These numbers are almost certainly higher for real soils because crystalline mineral assemblages can be much more complex than the mineral mixtures analyzed in this study, and structure models for crystalline minerals may not be appropriate or even available. In addition, organic matter, which can dominate the amorphous fraction of soils, may not be completely removed prior to PXRD analysis using H_2O_2, NaOCl, and $Na_2S_2O_8$ oxidants (Mikutta et al. 2005a) and thus significantly contribute to the determined iXAM fraction at very low iXAM concentrations, particularly in soil clay fractions (<2 μm) of organic matter-rich soil horizons. In this respect, our iXAM quantification results provide insight into what can be achieved by the Rietveld method under the best available conditions.

Based on Rietveld and XRF spectrometry results, the balance sheet method provided reasonably accurate data on the chemical iXAM composition in terms of major oxides for both sample preparation methods, even at iXAM contents as low as 10 wt% (Figs. 14 and 15; Online Materials[1] Tables S10 and S12). This further buttresses the efficiency of Rietveld method in quantifying and characterizing the chemical composition of soil iXAMs based on XRF data. However, our results also show that the balance sheet method may significantly overestimate minor oxides (<0.1 wt%) in iXAMs by up to 2.4 wt% (mean = 0.5 wt%) (Online Materials[1] Table S11). This was likely caused by small deviations between nominal and actual chemical compositions of crystalline minerals contained in the mineral mixtures and the intrinsic amorphicity or amorphicity induced in crystalline minerals during sample preparation. Therefore, oxide contents <3 wt% determined for soil iXAMs are highly uncertain and should be viewed with due caution. In general, the mass bias of oxide contents (Al_2O_3, CaO, Fe_2O_3, K_2O, MgO, Na_2O, SiO_2, TiO_2) of up to ±3 wt% derived from Rietveld and XRF analyses in our study was comparable to that obtained by full PXRD pattern fitting of soil samples combined with chemical analysis using inductively coupled plasma–mass spectrometry (Casetou-Gustafson et al. 2018).

The LOI of the ferrihydrite-opal mixture used in this study (15.3 wt%) contributed largely to the total LOI of all mineral mixtures analyzed (Online Materials[1] Table S9). This is a common phenomenon in soils, especially for iXAM-rich clay and silt fractions (Alexiades and Jackson 1966; Raman and Mortland 1969; Jones et al. 2000). Our results document that the balance sheet method leads to large relative LOI quantification errors of up to 371% for the iXAMs used (mean = 67.2%; Fig. 14, Online Materials[1] Table S12). This implies that LOI values determined for soil iXAMs become increasingly uncertain when iXAM contents are low and/or soil iXAMs possess an intrinsically low content of volatile elements such as ferrihydrite or opal-A (Online Materials[1] Fig. S3) as compared to, for example, short-range ordered aluminosilicates like allophane (Alexiades and Jackson 1966; Raman and Mortland 1969). Regardless of these restrictions, our results corroborate that the chemical composition of iXAMs in geomaterials in terms of major oxides can be accurately quantified using combined Rietveld and XRF analyses, irrespective of sample complexity and sample preparation method used for PXRD analysis.

IMPLICATIONS

Inorganic X-ray amorphous materials are a quantitatively important part of inorganic matter in soils (Blank and Fosberg 1991; Jones et al. 2000; Manaka 2006; Lessovaia et al. 2014, 2016), but analytical assessments of their quantification and chemical composition by QPA of PXRD data combined with chemical analyses are still lacking. Our results confirm that—independent of the sample preparation method—Rietveld analysis can provide accurate and precise data on iXAM contents in mineral mixtures resembling soils and other geomaterials. However, this requires a correct identification and an accurate quantification of all crystalline mineral phases present, which still poses a major challenge for soils containing high amounts of disordered clay minerals.

Our established analytical parameters and limitations of the Rietveld method for the quantification and chemical characterization of iXAMs in artificial mineral mixtures provide indispensable information for the quantification and chemical characterization of iXAMs in natural soils. In fact, information on the distribution and composition of iXAMs in soils of most world regions is completely lacking, although a large number of studies have highlighted the importance of iXAMs for soil physicochemical properties such as organic carbon and pollutant binding, soil aggregation, porosity, and plasticity (Goldberg 1989; Mikutta et al. 2005b; Rawlins et al. 2013; Lehtinen et al. 2014; Totsche et al. 2018; Lenhardt et al. 2022). In soil sciences, iXAMs such as ferrihydrite, silica, and short-range ordered aluminosilicates like allophane or imogolite are almost exclusively quantified by selective wet-chemical dissolution methods (Higashi and Ikeda 1974; Taylor and Schwertmann 1974; Walker 1983; Parfitt and Childs 1988; Wada 1989; Kaufhold et al. 2010). However, these methods are unable to assess the total abundance and chemical composition of soil iXAMs (Jones et al. 2000), especially when different kinds of iXAMs are present. QPA of PXRD data of soil samples in combination with elemental analysis, on the other hand, is currently the only method to reliably quantify total iXAM contents in soils and examine their chemical composition. This information is critical for establishing quantitative relationships between content and chemical composition of iXAMs and physicochemical properties and ecological functions of soils in the future.

Acknowledgments and funding

We are indebted to BGR for providing the minerals for this project and thank Claus Rüscher for assisting in the TG-DSC analyses. We are also greateful to Dominik Mock for SEM support. This work was funded by the German Research Foundation (DFG) (project no. 460744281).

References cited

Abollino, O., Malandrino, M., Giacomino, A., and Mentasti, E. (2011) The role of chemometrics in single and sequential extraction assays: A review: Part I. Extraction procedures, uni- and bivariate techniques and multivariate variable reduction techniques for pattern recognition. Analytica Chimica Acta, 688, 104–121, https://doi.org/10.1016/j.aca.2010.12.020.

Ahtee, M., Nurmela, M., Suortti, P., and Järvinen, M. (1989) Correction for preferred orientation in Rietveld refinement. Journal of Applied Crystallography, 22, 261–268, https://doi.org/10.1107/S0021889889000725.

Alexiades, C.A. and Jackson, M.L. (1966) Quantitative clay mineralogical analysis of soils and sediments. Clays and Clay Minerals, 14, 35–52, https://doi.org/10.1346/CCMN.1966.0140104.

Andrist-Rangel, Y., Simonsson, M., Andersson, S., Öborn, I., and Hillier, S. (2006) Mineralogical budgeting of potassium in soil: A basis for understanding standard measures of reserve potassium. Journal of Plant Nutrition and Soil Science, 169, 605–615, https://doi.org/10.1002/jpln.200621972.

Basile-Doelsch, I., Balesdent, J., and Rose, J. (2015) Are interactions between organic compounds and nanoscale weathering minerals the key drivers of carbon storage in soils? Environmental Science & Technology, 49, 3997–3998, https://doi.org/10.1021/acs.est.5b00650.

Bazilevskaya, E., Archibald, D.D., and Martínez, C.E. (2018) Mineral colloids mediate organic carbon accumulation in a temperate forest Spodosol: Depth-wise changes in pore water chemistry. Biogeochemistry, 141, 75–94, https://doi.org/10.1007/s10533-018-0504-4.

Bergmann, J., Kleeberg, R., and Taut, T. (1997) Quantitative phase analysis using a new Rietveld algorithm—assisted by improved stability and convergence behavior. Advances in X-ray Analysis, 40, 425.

Bergmann, J., Friedel, P., and Kleeberg, R. (1998) BGMN—A new fundamental parameters based Rietveld program for laboratory X-ray sources, its use in quantitative analysis and structure investigations. CPD Newsletter, 20, 5–8.

Bergmann, J., Monecke, T., and Kleeberg, R. (2001) Alternative algorithm for the correction of preferred orientation in Rietveld analysis. Journal of Applied Crystallography, 34, 16–19, https://doi.org/10.1107/S002188980001623X.

Bish, D.L. and Post, J.E. (1993) Quantitative mineralogical analysis using the Rietveld full-pattern fitting method. American Mineralogist, 78, 932–940.

Bish, D.L. and Reynolds, R.C. Jr. (1989) Sample preparation for X-ray diffraction. In D.L. Bish and J.E. Post, Eds., Modern Powder Diffraction, 20, p. 73–100. Reviews in Mineralogy and Geochemistry, Mineralogical Society of America, Chantilly, Virginia.

Blank, R.R. and Fosberg, M.A. (1991) Duripans of Idaho, U.S.A.: In situ alteration of eolian dust (loess) to an opal-A/X-ray amorphous phase. Geoderma, 48, 131–149, https://doi.org/10.1016/0016-7061(91)90012-I.

Brydon, J.E. and Shimoda, S. (1972) Allophane and other amorphous constituents in a podzol from Nova Scotia. Canadian Journal of Soil Science, 52, 465–475, https://doi.org/10.4141/cjss72-058.

Calvert C.S., Palkowsky D.A., and Pevear D.R. (1989) A combined X-ray powder diffraction and chemical method for the quantitative mineral analysis of geological samples. In D.R Pevear and F.A. Mumpton, Eds., Quantitative Mineral Analysis of Clays, p. 154–166. Clay Minerals Society, Workshop Lectures 5.

Casetou-Gustafson, S., Hillier, S., Akselsson, C., Simonsson, M., Stendahl, J., and Olsson, B.A. (2018) Comparison of measured (XRPD) and modeled (A2M) soil mineralogies: A study of some Swedish forest soils in the context of weathering rate predictions. Geoderma, 310, 77–88, https://doi.org/10.1016/j.geoderma.2017.09.004.

Cesarano, M., Bish, D.L., Cappelletti, P., Cavalcante, F., Belviso, C., and Fiore, S. (2018) Quantitative mineralogy of clay-rich siliciclastic landslide terrain of the Sorrento Peninsula, Italy, using a combined XRPD and XRF approach. Clays and Clay Minerals, 66, 353–369, https://doi.org/10.1346/CCMN.2018.064108.

Chipera, S.J. and Bish, D.L. (2002) FULLPAT: A full-pattern quantitative analysis program for X-ray powder diffraction using measured and calculated patterns. Journal of Applied Crystallography, 35, 744–749, https://doi.org/10.1107/S0021889802017405.

——— (2013) Fitting full X-ray diffraction patterns for quantitative analysis: A method for readily quantifying crystalline and disordered phases. Advances in Materials Physics and Chemistry, 3, 47–53, https://doi.org/10.4236/ampc.2013.31A007.

Chung, F.H. (1974) Quantitative interpretation of X-ray diffraction patterns of mixtures. I. Matrix-flushing method for quantitative multicomponent analysis. Journal of Applied Crystallography, 7, 519–525, https://doi.org/10.1107/S0021889874010375.

DeMumbrum, L.E. (1960) Crystalline and amorphous soil minerals of the Mississippi coastal terrace. Soil Science Society of America Journal, 24, 185–189, https://doi.org/10.2136/sssaj1960.03615995002400030018x.

Dietel, J., Gröger-Trampe, J., Bertmer, M., Kaufhold, S., Ufer, K., and Dohrmann, R. (2019a) Crystal structure model development for soil clay minerals—I. Hydroxy-interlayered smectite (HIS) synthesized from bentonite. A multi-analytical study. Geoderma, 347, 135–149, https://doi.org/10.1016/j.geoderma.2019.03.021.

Dietel, J., Ufer, K., Kaufhold, S., and Dohrmann, R. (2019b) Crystal structure model development for soil clay minerals—II. Quantification and characterization of hydroxy-interlayered smectite (HIS) using the Rietveld refinement technique. Geoderma, 347, 1–12, https://doi.org/10.1016/j.geoderma.2019.03.020.

Doebelin, N. and Kleeberg, R. (2015) Profex: A graphical user interface for the Rietveld refinement program BGMN. Journal of Applied Crystallography, 48, 1573–1580, https://doi.org/10.1107/S1600576715014685.

Dohrmann, R., Meyer, I., Kaufhold, S., Jahn, R., Kleber, M., and Kasbohm, J. (2002) Rietveld-based quantification of allophane. Mainzer Naturwissenschaftliches Archiv, 40, 28–30.

Dollase, W.A. (1986) Correction of intensities for preferred orientation in powder diffractometry: Application of the March model. Journal of Applied Crystallography, 19, 267–272, https://doi.org/10.1107/S0021889886089458.

Filgueiras, A.V., Lavilla, I., and Bendicho, C. (2002) Chemical sequential extraction for metal partitioning in environmental solid samples. Journal of Environmental Monitoring, 4, 823–857, https://doi.org/10.1039/b207574c.

Funk, W., Dammann, V., and Donnevert, G. (2005) Qualitätssicherung in der Analytischen Chemie, 2nd ed.. Wiley-VCH.

Goldberg, S. (1989) Interaction of aluminum and iron oxides and clay minerals and their effect on soil physical properties: A review. Communications in Soil Science and Plant Analysis, 20, 1181–1207, https://doi.org/10.1080/00103629009368144.

Gualtieri, A.F. (2000) Accuracy of XRPD QPA using the combined Rietveld RIR method. Journal of Applied Crystallography, 33, 267–278, https://doi.org/10.1107/S002188989901643X.

Gudmundsson, T. and Stahr, K. (1981) Mineralogical and geochemical alterations of "Podsol Bährhalde." Catena, 8, 49–68, https://doi.org/10.1016/S0341-8162(81)80004-5.

Hellmann, R., Eggleston, C.M., Hochella, M.F. Jr., and Crerar, D.A. (1990) The formation of leached layers on albite surfaces during dissolution under hydrothermal conditions. Geochimica et Cosmochimica Acta, 54, 1267–1281, https://doi.org/10.1016/0016-7037(90)90152-B.

Higashi, T. and Ikeda, H. (1974) Dissolution of allophane by acid oxalate solution. Clay Science, 4, 205–211.

Hillier, S. (1999a) Use of an air brush to spray dry samples for X-ray powder diffraction. Clay Minerals, 34, 127–135, https://doi.org/10.1180/000985599545984.

——— (1999b) Quantitative analysis of clay and other minerals in sandstones by X-ray powder diffraction (XRPD). In R.H. Worden and S. Morad, Eds., Clay Mineral Cements in Sandstones, 213–251. Wiley.

——— (2000) Accurate quantitative analysis of clay and other minerals in sandstones by XRD: Comparison of a Rietveld and a reference intensity ratio (RIR) method and the importance of sample preparation. Clay Minerals, 35, 291–302, https://doi.org/10.1180/000985500546666.

Järvinen, M. (1993) Application of symmetrized harmonics expansion to correction of the preferred orientation effect. Journal of Applied Crystallography, 26, 525–531, https://doi.org/10.1107/S0021889893001219.

Jones, R.C., Babcock, C.J., and Knowlton, W.B. (2000) Estimation of the total amorphous content of Hawai'i soils by the Rietveld method. Soil Science Society of America Journal, 64, 1100–1108, https://doi.org/10.2136/sssaj2000.6431100x.

Kaufhold, S., Ufer, K., Kaufhold, A., Stucki, J.W., Anastácio, A.S., Jahn, R., and Dohrmann, R. (2010) Quantification of allophane from Ecuador. Clays and Clay Minerals, 58, 707–716, https://doi.org/10.1346/CCMN.2010.0580509.

Kodama, H. and Wang, C. (1989) Distribution and characterization of noncrystalline inorganic components in spodosols and spodosol-like soils. Soil Science Society of America Journal, 53, 526–534, https://doi.org/10.2136/sssaj1989.03615995005300020037x.

Lehtinen, T., Lair, G.J., Mentler, A., Gísladóttir, G., Ragnarsdóttir, K.V., and Blum, W.E.H. (2014) Soil aggregate stability in different soil orders quantified by low dispersive ultrasonic energy levels. Soil Science Society of America Journal, 78, 713–723, https://doi.org/10.2136/sssaj2013.02.0073.

Lenhardt, K.R., Breitzke, H., Buntkowsky, G., Mikutta, C., and Rennert, T. (2022) Interactions of dissolved organic matter with short-range ordered aluminosilicates by adsorption and co-precipitation. Geoderma, 423, 115960, https://doi.org/10.1016/j.geoderma.2022.115960.

Lessovaia, S., Dultz, S., Goryachkin, S., Plötze, M., Polekhovsky, Y., Andreeva, N., and Filimonov, A. (2014) Mineralogy and pore space characteristics of traprocks from Central Siberia, Russia: Prerequisite of weathering trends and soil formation. Applied Clay Science, 102, 186–195, https://doi.org/10.1016/j.clay.2014.09.039.

Lessovaia, S.N., Plötze, M., Inozemzev, S., and Goryachkin, S. (2016) Traprock transformation into clayey materials in soil environments of the central Siberian plateau, Russia. Clays and Clay Minerals, 64, 668–676, https://doi.org/10.1346/CCMN.2016.064042.

Manaka, M. (2006) Amount of amorphous materials in relationship to arsenic, antimony, and bismuth concentrations in a brown forest soil. Geoderma, 136, 75–86, https://doi.org/10.1016/j.geoderma.2006.02.002.

McCusker, L.B., Von Dreele, R.B., Cox, D.E., Louër, D., and Scardi, P. (1999) Rietveld refinement guidelines. Journal of Applied Crystallography, 32, 36–50, https://doi.org/10.1107/S0021889898009856.

Mikutta, R., Kleber, M., Kaiser, K., and Jahn, R. (2005a) Review: Organic matter

removal from soils using hydrogen peroxide, sodium hypochlorite, and disodium peroxodisulfate. Soil Science Society of America Journal, 69, 120–135, https://doi.org/10.2136/sssaj2005.0120.

Mikutta, R., Kleber, M., and Jahn, R. (2005b) Poorly crystalline minerals protect organic carbon in clay subfractions from acid subsoil horizons. Geoderma, 128, 106–115, https://doi.org/10.1016/j.geoderma.2004.12.018.

Monecke, T., Kohler, S., Kleeberg, R., Herzig, P.M., and Gemmell, J.B. (2001) Quantitative phase-analysis by the Rietveld method using X-ray powder-diffraction data: Application to the study of alteration Halos associated with volcanic rock hosted massive sulfide deposits. Canadian Mineralogist, 39, 1617–1633, https://doi.org/10.2113/gscanmin.39.6.1617.

Omotoso, O., McCarty, D.K., Hillier, S., and Kleeberg, R. (2006) Some successful approaches to quantitative mineral analysis as revealed by the 3rd Reynolds Cup contest. Clays and Clay Minerals, 54, 748–760, https://doi.org/10.1346/CCMN.2006.0540609.

Parfitt, R. and Childs, C. (1988) Estimation of forms of Fe and Al—a review, and analysis of contrasting soils by dissolution and Mossbauer methods. Australian Journal of Soil Research, 26, 121–144, https://doi.org/10.1071/SR9880121.

Pospíšilová, Ľ., Uhlík, P., Menšík, L., Hlisnikovský, L., Eichmeier, A., Horáková, E., and Vlček, V. (2021) Clay mineralogical composition and chemical properties of Haplic Luvisol developed on loess in the protected landscape area Litovelské Pomoraví. European Journal of Soil Science, 72, 1128–1142, https://doi.org/10.1111/ejss.13041.

Raman, K.V. and Mortland, M.M. (1969) Amorphous materials in a spodosol: Some mineralogical and chemical properties. Geoderma, 3, 37–43, https://doi.org/10.1016/0016-7061(69)90044-5.

Rawlins, B.G., Wragg, J., and Lark, R.M. (2013) Application of a novel method for soil aggregate stability measurement by laser granulometry with sonication. European Journal of Soil Science, 64, 92–103, https://doi.org/10.1111/ejss.12017.

Rennert, T. (2019) Wet-chemical extractions to characterise pedogenic Al and Fe species—a critical review. Australian Journal of Soil Research, 57, 1–16, https://doi.org/10.1071/SR18299.

Rennert, T., Dietel, J., Heilek, S., Dohrmann, R., and Mansfeldt, T. (2021) Assessing poorly crystalline and mineral-organic species by extracting Al, Fe, Mn, and Si using (citrate-) ascorbate and oxalate. Geoderma, 397, 115095, https://doi.org/10.1016/j.geoderma.2021.115095.

Reynolds, R.C. Jr. (1989) Principles and techniques of quantitative analysis of clay minerals by X-ray powder diffraction. In D.R Pevear and F.A. Mumpton, Eds., Quantitative Mineral Analysis of Clays, p. 4–36. Clay Minerals Society Workshop Lectures 1.

Rietveld, H.M. (1969) A profile refinement method for nuclear and magnetic structures. Journal of Applied Crystallography, 2, 65–71, https://doi.org/10.1107/S0021889869006558.

Ross, G.J. (1980) Mineralogical, physical, and chemical characteristics of amorphous constituents in some podzolic soils from British Columbia. Canadian Journal of Soil Science, 60, 31–43, https://doi.org/10.4141/cjss80-004.

Ruiz-Agudo, E., Putnis, C.V., Rodriguez-Navarro, C., and Putnis, A. (2012) Mechanism of leached layer formation during chemical weathering of silicate minerals. Geology, 40, 947–950, https://doi.org/10.1130/G33339.1.

Ruiz-Agudo, E., King, H.E., Patiño-López, L.D., Putnis, C.V., Geisler, T., Rodriguez-Navarro, C., and Putnis, A. (2016) Control of silicate weathering by interface-coupled dissolution precipitation processes at the mineral-solution interface. Geology, 44, 567–570, https://doi.org/10.1130/G37856.1.

Sanborn, P., Lamontagne, L., and Hendershot, W. (2011) Podzolic soils of Canada: Genesis, distribution, and classification. Canadian Journal of Soil Science, 91, 843–880, https://doi.org/10.4141/cjss10024.

Scheffer, F. and Schachtschabel, P. (2010) Lehrbuch der Bodenkunde, 16th ed., 570 p. Spektrum Akademischer Verlag.

Schwertmann, U. and Taylor, R.M. (1972) The transformation of lepidocrocite to goethite. Clays and Clay Minerals, 20, 151–158, https://doi.org/10.1346/CCMN.1972.0200306.

Schwertmann, U., Schulze, D.G., and Murad, E. (1982) Identification of ferrihydrite in soils by dissolution kinetics, differential X-ray diffraction, and Mössbauer spectroscopy. Soil Science Society of America Journal, 46, 869–875, https://doi.org/10.2136/sssaj1982.03615995004600040040x.

Smith, S.T., Snyder, R.L., and Brownell, W.E. (1978) Minimization of preferred orientation in powders by spray drying. Advances in X-ray Analysis, 22, 77–87, https://doi.org/10.1154/S0376030800016426.

Szczerba, M. and Ufer, K. (2018) New model of ethylene glycol intercalate in smectites for XRD modelling. Applied Clay Science, 153, 113–123, https://doi.org/10.1016/j.clay.2017.12.010.

Tamppari, L.K., Anderson, R.M., Archer, P.D. Jr., Douglas, S., Kounaves, S.P., McKay, C.P., Ming, D.W., Moore, Q., Quinn, J.E., Smith, P.H., and others. (2012) Effects of extreme cold and aridity on soils and habitability: McMurdo Dry Valleys as an analogue for the Mars Phoenix landing site. Antarctic Science, 24, 211–228, https://doi.org/10.1017/S0954102011000800.

Tarrah, J., Meiwes, K.J., and Meesenburg, H. (2000) Normative calculation of minerals in North German loess soils using the modified CIPW norm. Journal of Plant Nutrition and Soil Science, 163, 307–312, https://doi.org/10.1002/1522-2624(200006)163:3<307:AID-JPLN307>3.0.CO;2-I.

Taylor, R.M. and Schwertmann, U. (1974) Maghemite in soils and its origin: I. Properties and observations on soil maghemites. Clay Minerals, 10, 289–298, https://doi.org/10.1180/claymin.1974.010.4.07.

Totsche, K.U., Amelung, W., Gerzabek, M.H., Guggenberger, G., Klumpp, E., Knief, C., Lehndorff, E., Mikutta, R., Peth, S., Prechtel, A., and others. (2018) Microaggregates in soils. Journal of Plant Nutrition and Soil Science, 181, 104–136, https://doi.org/10.1002/jpln.201600451.

Tsukimura, K. (1997) Crystallization of Al_2O_3–SiO_2 gels in water at 473 K. Mineralogical Journal, 19, 1–11, https://doi.org/10.2465/minerj.19.1.

Ufer, K., Roth, G., Kleeberg, R., Stanjek, H., Dohrmann, R., and Bergmann, J. (2004) Description of X-ray powder pattern of turbostratically disordered layer structures with a Rietveld compatible approach. Zeitschrift für Kristallographie. Crystalline Materials, 219, 519–527, https://doi.org/10.1524/zkri.219.9.519.44039.

Ufer, K., Stanjek, H., Roth, G., Dohrmann, R., Kleeberg, R., and Kaufhold, S. (2008) Quantitative phase analysis of bentonites by the Rietveld method. Clays and Clay Minerals, 56, 272–282, https://doi.org/10.1346/CCMN.2008.0560210.

Ufer, K., Kleeberg, R., Bergmann, J., and Dohrmann, R. (2012a) Rietveld refinement of disordered illite-smectite mixed-layer structures by a recursive algorithm. I: One-dimensional patterns. Clays and Clay Minerals, 60, 507–534, https://doi.org/10.1346/CCMN.2012.0600507.

——— (2012b) Rietveld refinement of disordered illite-smectite mixed-layer structures by a recursive algorithm. II: Powder-pattern refinement and quantitative phase analysis. Clays and Clay Minerals, 60, 535–552, https://doi.org/10.1346/CCMN.2012.0600508.

Ufer, K., Kleeberg, R., and Monecke, T. (2015) Quantification of stacking disordered Si-Al layer silicates by the Rietveld method: Application to exploration for high-sulphidation epithermal gold deposits. Powder Diffraction, 30, S111–S118, https://doi.org/10.1017/S0885715615000111.

Wada, K. (1989) Allophane and imogolite. In J.B. Dixon and S.B. Weed, Eds., Minerals in Soil Environments, p. 1051–1087. Soil Science Society of America.

Walker, A.L. (1983) The effects of magnetite on oxalate- and dithionite-extractable iron. Soil Science Society of America Journal, 47, 1022–1026, https://doi.org/10.2136/sssaj1983.03615995004700050036x.

Wang, X., Ufer, K., and Kleeberg, R. (2018) Routine investigation of structural parameters of dioctahedral smectites by the Rietveld method. Applied Clay Science, 163, 257–264, https://doi.org/10.1016/j.clay.2018.07.011.

Weidler, P.G., Luster, J., Schneider, J., Sticher, H., and Gehring, A.U. (1998) The Rietveld method applied to the quantitative mineralogical and chemical analysis of a ferralitic soil. European Journal of Soil Science, 49, 95–105, https://doi.org/10.1046/j.1365-2389.1998.00138.x.

Westphal, T., Füllmann, T., and Pöllmann, H. (2009) Rietveld quantification of amorphous portions with an internal standard–Mathematical consequences of the experimental approach. Powder Diffraction, 24, 239–243, https://doi.org/10.1154/1.3187828.

Zabala, S.M., Conconi, M.S., Alconada, M., and Torres Sánchez, R.M. (2007) The Rietveld method applied to the quantitative mineralogical analysis of some soil samples from Argentina. Ciencia del Suelo, 25, 65–73.

Zahoransky, T., Kaiser, K., and Mikutta, C. (2022) High manganese redox variability and manganate predominance in temperate soil profiles as determined by X-ray absorption spectroscopy. Geochimica et Cosmochimica Acta, 338, 229–249, https://doi.org/10.1016/j.gca.2022.10.016.

Žigová, A., Šťastný, M., and Kodešová, A. (2013) Development of soils on paragneiss and granite in the South-eastern part of Bohemia. Acta Geodynamica et Geomaterialia, 10, 85–95, https://doi.org/10.13168/AGG.2013.0008.

Manuscript received October 30, 2023
Manuscript accepted April 17, 2024
Accepted manuscript online May 1, 2024
Manuscript handled by Aaron J. Lussier

Endnote:

[1]Deposit item AM-24-129240. Online Materials are free to all readers. Go online, via the table of contents or article view, and find the tab or link for supplemental materials.